

Magnetic Materials for Quantum Magnonics

Rostyslav O. Serha,^{1, 2, a)} Carsten Dubs,³ and Andrii V. Chumak¹

¹⁾Faculty of Physics, University of Vienna, 1090 Vienna, Austria.

²⁾Vienna Doctoral School in Physics, University of Vienna, 1090 Vienna, Austria.

³⁾INNOVENT e.V. Technologieentwicklung, 07745 Jena, Germany.

(Dated: 12 February 2026)

Quantum magnonics studies the quantum properties of magnons—the quanta of spin waves—and their application in quantum information processing. Progress in this field depends on identifying magnetic materials with characteristics tailored to the diverse requirements of magnonics and quantum magnonics. For single-magnon excitation, its control, hybrid coupling, and entanglement, the most critical property is the ability to support long magnon lifetimes. This perspective reviews established and emerging magnetic materials—including ferromagnetic metals, Heusler compounds, antiferromagnets, altermagnets, organic and 2D van der Waals magnets, hexaferrites, europium chalcogenides, and in particular yttrium iron garnet (YIG)—highlighting their key characteristics. YIG remains the benchmark, with bulk crystals supporting sub-microsecond Kittel-mode lifetimes and ultra-pure spheres achieving $\sim 18 \mu\text{s}$ for dipolar-exchange magnons at millikelvin temperatures. However, thin YIG films on gadolinium gallium garnet (GGG) substrates suffer from severe lifetime reduction due to substrate-induced losses. In contrast, YIG films on a new lattice matched, diamagnetic alternative, yttrium scandium gallium/aluminum garnet (YSGAG), overcomes these limitations and preserves low magnetic damping down to millikelvin temperatures. These advances provide a practical pathway toward ultralong-living magnons in thin films, enabling scalable quantum magnonics with coherent transport, strong magnon-photon, magnon-qubit coupling, and integrated quantum networks.

I. INTRODUCTION INTO QUANTUM MAGNONICS

Quantum computing promises transformative advances in computation, with potential impacts on cryptography, materials science, and artificial intelligence^{1,2}. A central challenge for solid-state quantum technology is to identify an on-chip platform with a suitable nanoscale information carrier³. Magnons—the bosonic quanta of spin-wave excitations in ordered magnets—are promising for this role. The emerging field of quantum magnonics^{3–8} operates with quantum states of magnons, including single magnons, typically at millikelvin temperatures, where thermal magnons are suppressed. Magnons cover gigahertz to terahertz frequencies⁹, scale to nanometer footprints^{10,11}, interface naturally with microwave circuitry¹², and exhibit strongly nonlinear and nonreciprocal dynamics^{13–17}. These properties position magnons as promising candidates for quantum information processing, coherent transport, and entangled-state preparation^{3–7}.

At room temperature (RT), macroscopic quantum phenomena in magnon gases are already accessible. Theory and experiment have established Bose–Einstein condensation of magnons^{18–21}, magnonic supercurrents^{22,23}, and the magnonic Aharonov–Casher effect^{24,25}. In antiferromagnets, quantum magnonics can reach the terahertz regime. Cavity-coupled antiferromagnetic magnons have been demonstrated in collinear and canted phases²⁶, and terahertz cavity magnon polaritons have been realized in prototype platforms²⁷. Long-distance coherent antiferromagnetic spin-wave propagation at RT further supports device scaling viability²⁸. These advances complement broader arguments for magnons as quantum excitations with frequency tunability

and compatibility with hybrid architectures^{3,5,7,8}.

Single-magnon operations in ferromagnetically ordered media require suppression of thermal magnon populations. At a frequency of 4 GHz, which is typical for superconducting qubits and sufficiently high to forbid three-magnon splitting while providing longer lifetimes than at higher frequencies where viscous damping is stronger²⁹, the thermal magnon occupation can be kept below 0.01 according to Bose–Einstein statistics only if experiments are performed in dilution refrigerators at temperatures of about 40 mK or lower³⁰. The objective is to generate, control, and read out single magnons in hybrid systems that couple to photons, microwave cavities, phonons, or superconducting qubits^{31–35}.

Theory identifies roles for magnons as quantum interconnects and as probes of solid state quantum effects^{36–39}. Further proposals predict steady state magnon squeezing and photon-magnon entanglement in cavity hybrids using Kerr nonlinearities and engineered couplings^{40–44}. Magnomechanical schemes show how squeezing can enhance correlations and light-matter control and enable nonclassical state preparation^{45,46}. Experimentally, key milestones include coherent coupling of fundamental magnon modes to superconducting resonators^{4,6,47}, qubit based quantum sensing³², single magnon detection with a superconducting qubit³³, full Wigner function tomography of a single magnon⁴⁸, macroscopic Bell state between a spin system and a superconducting qubit⁴⁹, and NV-based platforms that quantify magnon mediated NV-NV coupling^{50,51}. Although the best Kittel-mode magnon lifetimes^{33,48} of several hundred nanoseconds are shorter than the decoherence times of state-of-the-art superconducting qubits, which reach tens of microseconds⁵², they are sufficient for entanglement transfer and for interfacing heterogeneous quantum systems^{4,5,7,8,31}. Recently, a qubit-free approach to quantum magnonics has been proposed, where Gaussian quantum states of ferromagnetic resonance magnons, including squeezed⁵³ and entangled states,

^{a)} Author to whom correspondence should be addressed:
rostyslav.serha@univie.ac.at

are generated via parametric driving and magnonic nonlinearities, enabling quantum-state preparation and verification using conventional ferromagnetic resonance techniques⁵⁴.

The most recent single-magnon experiments have been carried out on bulk spheres of yttrium iron garnet (YIG)^{33,48,49}, which provides the longest coherence with Kittel-mode lifetimes generally below one microsecond⁵⁵, underscoring its importance as the leading platform for quantum magnonics. Significant progress has been made in extending lifetimes at low temperatures, at which in ultra-pure bulk YIG, dipolar-exchange magnons reach about 18 μ s at millikelvin temperatures⁵⁶.

A central challenge in integrating superconducting qubits with magnetic resonant systems is the strong sensitivity of conventional qubits to external magnetic fields, which significantly reduces their coherence times. Such fields are, however, required to tune magnetic resonators to microwave frequencies relevant for quantum applications. For instance, the Kittel mode of a YIG sphere at 4 GHz requires an external magnetic field of approximately 150 mT, a field strength that typical aluminum-based superconducting qubits cannot tolerate. Current experimental approaches therefore rely on spatially separating the magnetic resonator and the superconducting qubit, coupling them indirectly via a microwave cavity mode. This allows the YIG sphere to be biased by a magnetic field while keeping the qubit in a field-free environment^{33,48,49}. This strategy could be further improved by employing planar superconducting resonators fabricated from materials that are more tolerant to magnetic fields such as niobium, niobium-tin or niobium-titanium, or by using qubits intrinsically robust against moderate magnetic fields^{57–59}. An alternative route is the use of magnetic waveguides as magnonic media operating at or near zero external field. YIG waveguides have already demonstrated operation at frequencies around 1.7 GHz⁶⁰. Upon cooling to cryogenic temperatures, the increase in saturation magnetization⁶¹ is expected to shift this frequency upward to approximately 3 GHz, placing it within a range that is well compatible with commonly engineered superconducting qubits.

Scaling from localized resonators to circuit-level links requires propagating magnons. Propagation enables spatial separation of single-magnon sources and detectors, and allows the transport of quantum states across a chip^{62–64}. This shifts attention from bulk magnetic resonators to thin films, where dipolar-driven magnons can travel. However, thin films perform worse than bulk samples, as their higher surface-to-volume ratio enhances the effect of surface defects. A further challenge in thin YIG films arises from the paramagnetism of GGG substrates at low temperatures^{65–70}. This limitation has recently been overcome by growing YIG films on a newly developed lattice-matched diamagnetic substrate^{71,72}. These advances enable on-chip platforms that excite and detect propagating magnons with planar resonators¹⁴. They also connect to ultralow-temperature studies of damping in bulk YIG^{56,70}, to wavenumber-dependent damping in films⁷³, and to nanoscale propagation at cryogenic temperatures⁶⁴. Together, this progress establishes a foundation for quantum magnonic circuits that integrate superconducting qubits, pho-

tons, and phonons, and exploit the nonlinear and nonreciprocal dynamics of magnons^{3,74–76}.

II. AVAILABLE MAGNETIC MATERIALS

Magnonics relies on ordered magnetic media that efficiently support spin waves. In this Perspective, we briefly present and analyze different material platforms, including those that have been widely used for many years as well as more recent and highly attractive candidates. An overview is provided in Tab. I, and representative examples are illustrated in Fig. 1. Further, the magnon lifetime in the discussed materials is commonly extracted from resonance measurements of the fundamental Kittel mode. The full width at half maximum (FWHM) ΔB of the magnetic resonance quantifies the magnetic losses of the system and allows one to determine the lifetime τ of the magnetic excitation via

$$\tau = \frac{1}{\gamma \cdot \Delta B}, \quad (1)$$

where γ is the gyromagnetic ratio²⁹. When comparing magnon damping and lifetimes across different magnetic materials, it is important to distinguish between the phenomenological Gilbert damping parameter α and the actual lifetime τ of a magnonic excitation. While α provides a convenient description of viscous damping in the Landau–Lifshitz–Gilbert framework and is commonly extracted from resonance linewidths, it does not uniquely determine magnon lifetimes in general. The magnetic linewidth ΔB of a system is related to the Gilbert damping parameter α by

$$\Delta B(f) = \Delta B_0 + \frac{4\pi\alpha}{\gamma} f, \quad (2)$$

where ΔB_0 denotes the inhomogeneous linewidth broadening, corresponding to the linearly extrapolated linewidth at zero frequency ($f = 0$).

In practice, linewidth broadening and magnon relaxation can arise from a variety of mechanisms beyond intrinsic viscous Gilbert damping, including impurity scattering, two-magnon scattering, magnon–phonon coupling, and slow-relaxor processes on rare-earth and L -state transition metal ion impurities, the latter being particularly relevant in YIG at cryogenic temperatures^{29,77}. As a result, linewidth measurements may deviate substantially from those expected from a simple linear Gilbert damping picture, especially when comparing different magnon wavelengths, temperature regimes, or material classes.

In antiferromagnets, the role of Gilbert damping and its relation to magnon lifetimes differ significantly from those in ferro- and ferrimagnets due to the two-sublattice nature of the magnetic order¹⁰⁷. The dynamics are governed by the Néel order parameter and described by inertial equations of motion, with damping entering as a matrix rather than as a single scalar parameter^{108,109}. Consequently, direct comparisons of Gilbert damping parameters across different magnetic orders are generally not meaningful without accounting for the underlying

TABLE I. Comparison of magnetic media relevant to quantum magnonics.

Property	YIG 55,56,61,78–83	Permalloy (Py) ^{84–87}	CoFeB 17,88–90	Hematite 28,91–93	Hexaferrite BaM ^{94–98}	Heusler CMFS ^{99–102}	CrPS 103–106
Chemical composition	Y ₃ Fe ₅ O ₁₂	Ni ₈₁ Fe ₁₉	Co ₄₀ Fe ₄₀ B ₂₀	Fe ₂ O ₃	BaFe ₁₂ O ₁₉	Co ₂ Mn _{0.6} Fe _{0.4} Si	CrPS ₄
Structure	single-crystalline	polycrystalline	amorphous	single-crystalline	single-crystalline	single-crystalline	2D van der Waals
Gilbert damping α	3×10^{-5}	7×10^{-3}	4×10^{-3}	5×10^{-5}	7×10^{-4}	3×10^{-3}	1×10^{-2} ^a
Saturation magnetization @ RT M_s (kA/m)	140	800	1250	—	320-390	1000	—
Exchange constant @ RT A (pJ/m)	3.6	16	15	10–20	6-9	13	10 ^a
Curie (Néel) temperature $T_{c(N)}$ (K)	560	550–870	1000	950	726	> 985	37

^a Used in micromagnetic simulations¹⁰⁶.

relaxation mechanisms. Therefore, in this Perspective we focus on direct linewidth measurements of magnetic excitations in ferro- and ferrimagnets as a more reliable measure of the actual magnon lifetime.

Ferromagnetic metals

A common class of materials used to excite spin waves is ferromagnetic metals, valued for their straightforward fabrication, compatibility with standard nanofabrication techniques, and high saturation magnetization, which enables efficient spin-wave excitation and access to large frequency bandwidths (see Tab. I). Prominent examples include Permalloy (Ni₈₁Fe₁₉)^{84,85,87}, CoFeB (Co₄₀Fe₄₀B₂₀)^{17,88–90,110,111}, and CoFe¹¹². In particular, propagating spin-wave spectroscopy on epitaxial single-crystal Fe thin films revealed an effective Gilbert damping as low as $\alpha \approx 2.5 \times 10^{-3}$, with lifetimes of up to 2 ns¹¹³. Even lower intrinsic damping has been demonstrated in carefully engineered CoFe alloys, where Gilbert damping values down to $\alpha \approx 5 \times 10^{-4}$ were reported¹¹². This reduction is attributed to a minimum in the electronic density of states at the Fermi level, which suppresses magnon–electron scattering and highlights the role of band-structure engineering in controlling dissipation in metallic systems. Their relatively large exchange stiffness and saturation magnetization further allow for short-wavelength magnons and high group velocities, advantageous for compact device architectures and broadband operation⁹.

At the same time, the presence of itinerant electrons in ferromagnetic metals introduces intrinsic dissipation channels through electron–magnon and electron–phonon scattering, resulting in magnetic damping that typically limits magnon lifetimes to the nanosecond regime¹¹⁴. Despite short lifetimes ferromagnetic metals remain relevant for cryogenic magnonics and hybrid quantum platforms, particularly in regimes requiring fast dynamics, large saturation magnetization, electrical tunability, strong nonlinearities, or strong coupling to

microwave photons¹¹⁵. Their metallic nature enables efficient electrical control via spin-transfer and spin–orbit torques and supports rapid energy exchange in strongly coupled hybrid systems, facilitating the integration of magnonic and electronic functionalities on a single chip⁸.

Heusler compounds

Heusler compounds, a class of mostly ternary or quaternary intermetallics with highly tunable electronic and magnetic properties^{118–120}, offer an improvement over conventional metallic ferromagnets by combining high spin polarization, large saturation magnetization, and comparatively low magnetic damping. Among the most studied in the magnonics and spintronics communities are Co₂-based full Heusler alloys, where half-metallic electronic structures and high crystalline order can suppress magnon dissipation channels¹²¹.

A particularly promising example is the quaternary Heusler compound CMFS (Co₂Mn_{0.6}Fe_{0.4}Si), for which low-damping spin-wave propagation and extended lifetimes have been demonstrated experimentally^{102,122}. Thin film studies of CFMS and related Co₂FeGa_{0.5}Ge_{0.5} (CFGG) alloys report effective Gilbert damping parameters in the range of $\alpha_{\text{eff}} \sim 10^{-3}$ to 10^{-2} , with evidence for both intrinsic and extrinsic damping contributions, such as two-magnon scattering¹²³. Additionally, substrate engineering has been shown to reduce Gilbert damping in CFAS (Co₂FeAl_{0.5}Si_{0.5}) Heusler films, with optimal annealing conditions yielding α values significantly lower than in as-grown films¹²⁴.

Furthermore, theoretical and experimental studies on Co₂MnZ (Z = Si, Ge, Sn, Sb) Heusler systems have identified pathways toward ultralow magnetic damping ($\alpha \sim 4 \times 10^{-4}$ – 9×10^{-4}), representing some of the lowest values reported for metallic ferromagnets and highlighting the crucial role of spin polarization and Fermi-level band structure in damping reduction¹²¹. More recently, ultra-low magnetic damping has been demonstrated in epitaxial Co₂MnSi Heusler

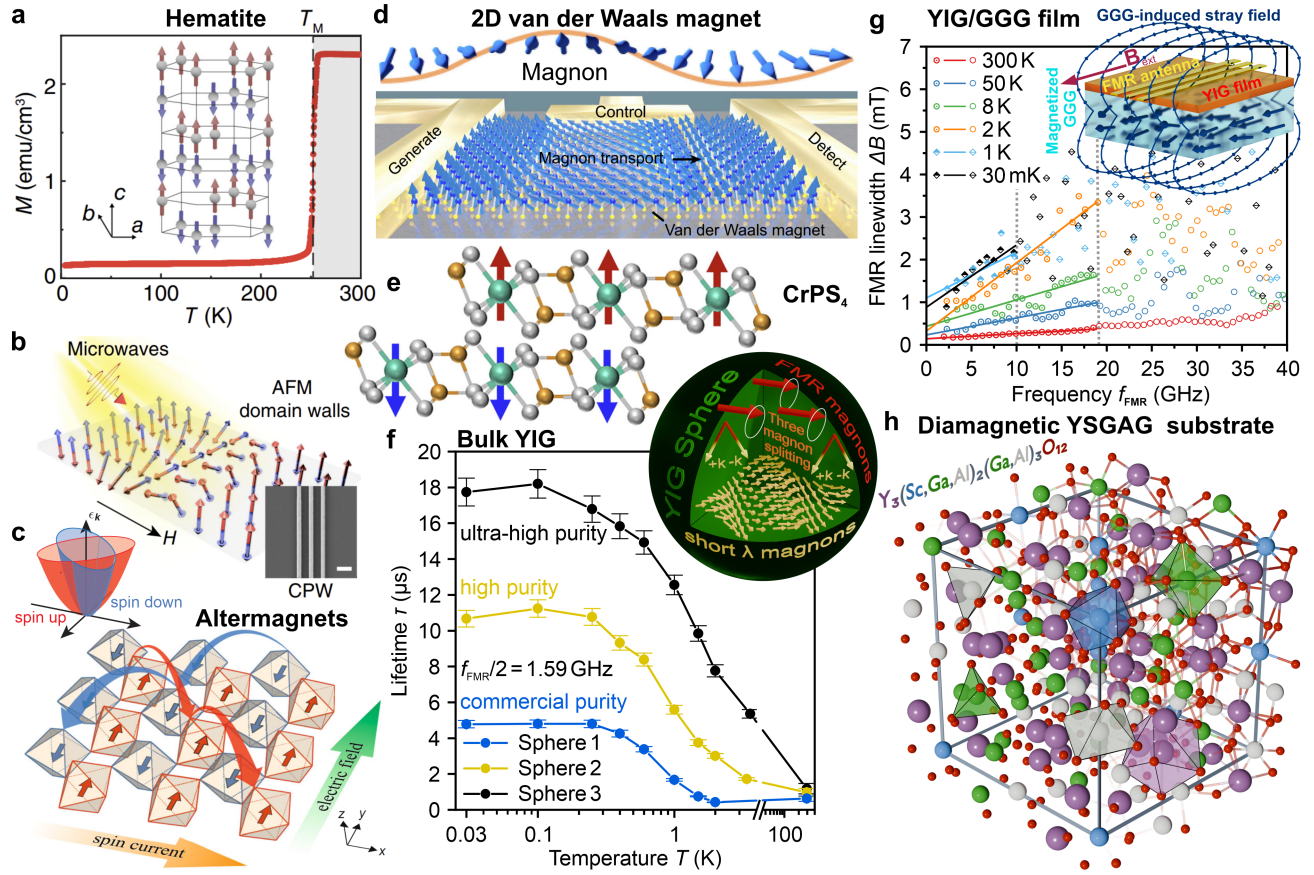


FIG. 1. (a) Temperature-dependent magnetization of hematite. Inset shows the easy-axis crystal structure for $T < T_M$ ⁹¹. Reproduced with permission from J. Chen *et al.*, *Phys. Rev. Lett.* **134**, 056701 (2025). Copyright 2025 American Physical Society. (b) Sketch of the antiferromagnetic (AFM) spin texture under microwave excitation. The magnetic field is applied along the x direction. Inset shows a SEM image of the coplanar waveguide (CPW); scale bar 500 nm⁹¹. Reproduced with permission from J. Chen *et al.*, *Phys. Rev. Lett.* **134**, 056701 (2025). Copyright 2025 American Physical Society. (c) Altermagnet: d -wave-type spin-split bands (upper left) and perovskite schematic with sublattice-dependent, anisotropic spin-dependent hoppings (red/blue arrows)¹¹⁶. Reproduced from M. Naka *et al.*, *npj Spintronics* **3**, 1 (2025), licensed under a Creative Commons Attribution–NonCommercial–NoDerivatives 4.0 International License. (d) Illustration of spin waves in a 2D van der Waals magnet. Magnon spintronics relies on manipulation and control of magnon spin transport from an injector to a detector. The electrical contacts for generating, controlling, and detecting magnons are shown as gold pads, while the van der Waals magnet is depicted by blue and yellow atoms (magnetic and non-magnetic, respectively). The spin is represented by a blue arrow whose orientation varies spatially to indicate the transported magnon¹¹⁷. Reproduced from S. Mañas-Valero *et al.*, *Fundamentals and applications of van der Waals magnets in magnon spintronics*, *Newton* **1**, 100018 (2025). Copyright Elsevier (2025). (e) Atoms and spins in a bilayer of the van der Waals antiferromagnet CrPS₄. Red and blue arrows indicate the local magnetic moments of the Cr atoms (turquoise). The interlayer (intralayer) exchange coupling is ferromagnetic (antiferromagnetic)¹⁰³. Reproduced with permission from D. K. de Wal *et al.*, *Phys. Rev. B* **107**, L180403 (2023). Copyright 2023 American Physical Society. (f) Lifetime τ of secondary dipolar–exchange magnons (DESW) at $f_{\text{FMR}}/2$ as a function of temperature T (logarithmic T -axis) for three YIG spheres. The purity of the YIG samples with respect to rare-earth ion impurities increases from commercial standard purity in Sphere 1 to ultra-high purity in Sphere 3. Illustration shows a schematic of three-magnon splitting—the $k = 0$ uniform mode ($f_{\text{FMR}} = 3.17$ GHz) splits into two counter-propagating magnons at 1.59 GHz with $|k| \approx 3 \text{ rad}\mu\text{m}^{-1}$ in the dipolar–exchange spin-wave regime⁵⁶. Reproduced from R. O. Serha *et al.*, arXiv:2505.22773 (2025); licensed under a Creative Commons Attribution 4.0 International (CC BY) license. (g) Experimental FMR linewidth Δf as a function of the FMR frequency f_{FMR} for a 100 nm YIG film on a GGG substrate. The half-solid points are measurement points up to 18 GHz for temperatures above 2 K and up to 10 GHz for temperatures below 2 K (gray dashed lines mark these limits). The straight lines are Gilbert fits performed up to 18 GHz and 10 GHz, respectively. Above these values, the linewidth shows non-Gilbert behavior versus f_{FMR} . The linewidth broadening and deviation from Gilbert behavior are due to magnetization of the GGG substrate at low temperatures (inset), which creates an inhomogeneous stray field affecting the internal field of the YIG film⁶⁵. Reproduced from R. O. Serha *et al.*, *Materials Today Quantum* **5**, 100025 (2025); licensed under a Creative Commons Attribution 4.0 International (CC BY) license. (h) Crystal structure of diamagnetic YSGAG, an alternative substrate to paramagnetic GGG for YIG. The cubic lattice structure of YSGAG is similar to that of YIG, but with iron ions replaced at the octahedral sites by scandium, gallium, and aluminum, while tetrahedral sites are occupied by gallium and aluminum⁷². Reproduced from R. O. Serha *et al.*, arXiv:2508.19044 (2025); licensed under a Creative Commons Attribution–NonCommercial–NoDerivatives 4.0 International (CC BY-NC-ND) license.

thin films, where transport measurements revealed a strong correlation between crystalline order, spin polarization, and reduced magnon dissipation, underscoring the potential of highly ordered Heusler alloys for low-loss magnon transport down to cryogenic temperatures¹²⁵. In addition, other Co-based Heusler compounds, such as CoFe_2Al , have also been reported to exhibit relatively low magnetic damping, suggesting a broader materials landscape for low-loss metallic magnonics¹²⁶.

Despite these improvements relative to conventional ferromagnetic metals, Heusler compounds still possess finite electrical conductivity, which continues to provide intrinsic dissipation channels via electron–magnon and electron–phonon scattering. Consequently, magnon lifetimes in optimized Heusler systems remain in the nanosecond regime. As a result, Heusler compounds represent an attractive and versatile materials platform for magnonics and spintronics, particularly in hybrid device architectures and electrically controlled magnon transport, while ongoing advances in materials optimization continue to expand their potential for long-lived quantum magnon applications.

Antiferromagnets

Antiferromagnets have emerged as a promising platform for magnonics and quantum magnonics, driven by a series of recent theoretical advances. Foundational work has shown that antiferromagnetic insulators can support superfluid spin transport, enabling coherent long-range spin currents without net magnetization¹²⁷. Their rich spin textures and ultrafast dynamics further highlight the potential of antiferromagnets for spintronic and magnonic devices¹⁰⁷. More recently, the quantum aspects of antiferromagnetic magnons have been explored. In this context, a transmon qubit has been proposed as a probe of their quantum characteristics¹²⁸. In parallel, spin–orbit interaction has been predicted to mediate the hybridization of antiferromagnetic magnons with plasmons, i.e., collective charge-density oscillations of conduction electrons, resulting in coherently coupled magnon–plasmon modes with modified dispersions and nontrivial band topology described within a quantum-mechanical framework¹²⁹.

A representative antiferromagnet of growing interest in magnonics is hematite^{130–132} ($\alpha\text{-Fe}_2\text{O}_3$) and shown in Fig. 1 (a). Bulk studies at GHz frequencies report low Gilbert damping (see Tab. I)^{28,91,92}. In the easy-axis phase below the Morin transition, all-electrical spectroscopy reveals nearly gapless antiferromagnetic magnons bound to 180° domain walls that propagate over micrometre distances with a group velocity of about 6 km/s, as illustrated in Fig. 1 (b). The domain-wall mode exhibits a full width at half maximum (FWHM) frequency linewidth $\Delta f_{\text{FWHM}} \approx 1.2$ GHz and a corresponding lifetime $\tau \approx 0.3$ ns⁹¹. Another canted antiferromagnet with even better damping characteristics is yttrium orthoferrite (YFeO_3)¹³³. It exhibits linewidths below 10 mT at frequencies around 350 GHz and a temperature of 20 K, corresponding to magnon lifetimes slightly above one nanosecond. Although antiferromagnets can reach terahertz frequen-

cies, which push the quantum regime to higher temperatures (e.g. 1 THz \approx 48 K), the relatively short lifetimes currently limit the use of hematite, YFeO_3 and other antiferromagnets for quantum magnonics.

Altermagnets

Recently, altermagnets have emerged as a distinct class of magnetic materials beyond conventional ferro- and antiferromagnets (see Fig. 1 (c)), characterized by compensated collinear order in real space and non-relativistic alternating spin splitting in momentum space^{134,135}. This unique duality yields terahertz-frequency, field-robust dynamics with negligible stray fields—features reminiscent of antiferromagnets—while also enabling spin-polarized band structures and novel transport phenomena, such as the crystal anomalous Hall effect, the spin-splitter effect, and anisotropic magnon spectra. Depending on the orbital symmetry of the momentum-dependent spin splitting, altermagnets are classified into even-parity (d-, g- and i-wave) orders with nodal sign changes (e.g., d-wave materials^{134,136} like RuO_2 ¹³⁵, MnTe ¹³⁷). They are distinguished from s- and p-wave (odd or no-node) patterns found in ferromagnets or antiferromagnets. A prominent example is hematite ($\alpha\text{-Fe}_2\text{O}_3$), a well-established antiferromagnet in magnonics^{28,91,92,131,132}, which has recently been identified as an altermagnet and shown to host anisotropic magnon excitations consistent with momentum-dependent spin splitting^{138,139}. Altogether, this makes altermagnets attractive for quantum magnonics, although the reduced lifetimes due to magnon–magnon interactions¹⁴⁰ should be taken into account, as is the case for antiferromagnets.

2D van der Waals and organic magnets

Recently, two-dimensional (2D) van der Waals magnets, illustrated in Fig. 1 (d) and (e), have attracted renewed interest in magnonics¹⁴¹. A notable example is the van der Waals antiferromagnet CrPS_4 (see Tab. I and Fig. 1 (e)), which supports long-distance magnon transport¹⁰³. Likewise, van der Waals magnets, such as CrCl_3 exhibit standing spin waves. Experiments resolve modes across a thickness of 20 μm , demonstrating control of spin-wave modes in 2D systems¹⁴². On the theoretical side, theory shows that dipolar interactions strongly shape magnon dispersion and edge-localized modes in two-dimensional van der Waals ferromagnets¹⁴³. Propagating spin waves have been detected in the 2D van der Waals ferromagnet Fe_5GeTe_2 , despite relatively high magnetic damping¹⁴⁴. In addition, recent advances in materials engineering have demonstrated that interfacial control can substantially enhance the magnetic properties of van der Waals magnets, as exemplified by wafer-scale Fe_4GeTe_2 films exhibiting robust ferromagnetism far above room temperature, emphasizing the potential of interface engineering to tailor magnetic order and magnonic properties in two-dimensional systems¹⁴⁵. These

results highlight 2D materials as tunable and versatile platforms for future magnonic applications.

Organic magnets also offer promise through chemical tunability and potentially low-damping propagation. For example, $V(\text{TCNE})_x$ exhibits lifetimes up to 40 ns^{146,147}. Low magnetic damping, together with their other advantageous properties, makes these materials highly promising for quantum magnonics. Further research is needed to fully understand and explore their potential.

Hexaferrites

For long magnon lifetimes and extended free paths, it is essential to use electrically insulating materials to eliminate the dissipation channel from magnons into free electrons. A prominent class of such magnetic insulators are the M-type hexaferrites, with barium hexaferrite ($\text{BaFe}_{12}\text{O}_{19}$, BaM) as their flagship representative. BaM is an insulating ferrimagnet with robust performance across a wide temperature range ($T_C \approx 725 \text{ K}$)⁹⁵, high coercivity and remanence, and a saturation magnetization of $M_s \approx 380 \text{ kA/m}$ at RT⁹⁵. Its strong intrinsic magnetic anisotropy ($H_a \approx 1353 \text{ kA/m}$) enables broadband frequency operation (50–65 GHz in undoped films at low magnetic fields⁹⁴, and 20–100 GHz in doped films⁹ under moderate biasing magnetic fields $< 0.8 \text{ T}$), as well as comparatively low magnetic losses (Gilbert damping constants as low as $\alpha \sim 7 \times 10^{-4}$)^{96,148}.

BaM supports spin waves with high group velocities, while its strong perpendicular magnetic anisotropy permits isotropic forward-volume spin-wave propagation in the film plane already under low external magnetic bias. Combined with intrinsically low magnetic damping, with Gilbert damping constants on the order of $\alpha \sim 10^{-4}$, these properties make BaM a highly attractive material for magnonic radio-frequency (RF) signal processing and data-processing applications, including operation in the 5G FR2 frequency range (24.25–71.0 GHz)^{9,149}. BaM uniquely enables magnonic access to technologically relevant frequency bands above 60 GHz that are difficult to reach with other ferrimagnets. These include the 60 GHz band used for in-cabin automotive radar and health-monitoring applications¹⁵⁰, as well as the 76–81 GHz band employed in long-range automotive radar systems¹⁵¹. Importantly, the large uniaxial anisotropy enables self-magnetized operation, allowing access to high-frequency magnonic modes with little or no external bias field. In nm-thick BaM waveguides, the fundamental spin-wave frequencies naturally lie in the tens-of-GHz range. These frequencies are primarily set by the internal anisotropy field rather than an applied magnetic field.

By providing high-frequency and potentially field-free spin-wave operation, BaM positions magnonics as a viable and competitive platform for next-generation RF signal processing and sensing technologies, enabling contributions to application domains that remain inaccessible to conventional magnonic materials. At the same time, the intrinsically high operating frequencies and low damping of BaM make this material class a promising candidate for high-frequency quantum

magnonics, where large magnon energies are advantageous for suppressing thermal occupation in quantum magnonics. The main limitation of BaM for modern magnonics arises from the absence of lattice-matched growth techniques capable of producing high-quality single-crystal nanoscale films that simultaneously provide low magnetic loss, low bias fields, and high-frequency performance. Systematic studies of BaM at cryogenic temperatures are therefore highly desirable and remain largely unexplored.

Europium Chalcogenides

A class of magnetic insulators and semiconductors that become magnetically ordered only at cryogenic temperatures — and are therefore unsuitable for room-temperature magnonics and spintronics, yet potentially relevant for quantum magnonics — are the europium chalcogenides ($\text{Eu}^{2+}\text{X}^{2-}$)^{152–155}. This material family includes europium oxide (EuO), europium sulfide (EuS), europium selenide (EuSe), and europium telluride (EuTe). All compounds crystallize in the rock-salt structure and exhibit band gaps ranging from approximately 1.2 eV (EuSe) to about 2.4 eV (EuTe), making them model systems for studying localized Heisenberg magnetism driven by 4f electrons¹⁵⁶.

The magnetic order in europium chalcogenides is governed by nearest- and next-nearest-neighbor exchange interactions, resulting in ferromagnetic ground states in EuO and EuS with Curie temperatures of $T_C \approx 69 \text{ K}$ and $T_C \approx 16.6 \text{ K}$, respectively. In contrast, EuSe exhibits a complex antiferromagnetic ground state below $T_N \approx 4.6 \text{ K}$ with field-induced metamagnetic phases that depend sensitively on temperature and external magnetic field, while EuTe is an antiferromagnet with a Néel temperature of $T_N \approx 9.6 \text{ K}$. Owing to the large magnetic moment of the Eu^{2+} ion ($S = 7/2$), these materials exhibit exceptionally high saturation magnetizations, reaching approximately 1900 kA/m in EuO and about 1300 kA/m in EuTe (in the fully field-saturated antiferromagnetic state). As a result, spin-wave frequencies in europium chalcogenides are significantly higher than in most conventional magnetic insulators.

Magnetic damping and resonance linewidths in europium chalcogenides have been investigated primarily at low temperatures using ferromagnetic and antiferromagnetic resonance techniques. In high-quality single crystals, remarkably narrow linewidths have been reported, with values on the order of millitesla for EuS, while comparable or slightly larger low-temperature linewidths have been observed in EuO, EuSe, and EuTe depending on the magnetic phase and field configuration^{157–163}. Taking the lowest reported linewidth for EuS, $\Delta B \approx 1 \text{ mT}$ at $T \approx 1.4 \text{ K}$ and microwave frequencies around 22 GHz, yields a magnon lifetime of approximately $\tau \approx 6 \text{ ns}$ ¹⁵⁸.

EuS has recently been employed in studies of magnon transport driven by the spin Seebeck effect in ferromagnetic EuS thin films¹⁶⁴, demonstrating its relevance for cryogenic magnonics. While the magnon lifetimes in europium chalcogenides are currently much shorter than those achieved in quantum magnonics experiments based on YIG, they are already comparable to coherence times relevant for hy-

brid quantum systems operating in the few-gigahertz regime. Given the localized 4f magnetism, the absence of itinerant charge carriers, and the presence of strong exchange fields, further improvements in linewidth and magnon lifetime may be expected in defect-reduced samples and at millikelvin temperatures. These considerations position europium chalcogenides as a promising, yet largely unexplored, materials platform for quantum magnonics and motivate systematic investigations of their magnon lifetimes, coherence properties, and dissipation mechanisms in the quantum limit.

Yttrium Iron Garnet

The longest magnon lifetimes have so far been achieved in YIG, which remains the only material particularly used for single-magnon excitation, measurement, and manipulation. This outstanding material is a ferrimagnetic insulator^{55,78} has a well understood magnetization behavior⁶¹ and magnetic anisotropy¹⁶⁵. The damping of coherent magnons arises primarily from scattering on crystallographic and surface defects^{166,167}, from rare-earth impurities^{56,69,77,168,169}, and from interactions with thermal magnons^{170,171} (spin-spin interaction) and phonons^{172–179} (spin-lattice interaction). As summarized in Tab. II, for example at millikelvin temperatures, an FMR linewidth of 0.02 mT corresponds to a magnon lifetime of about 300 ns⁵⁶, i.e., the minimally required timescale of a few hundred nanoseconds for single-magnon experiments^{33,48}. Even so, lifetimes of this order are still sufficient to sustain spin-wave coherence for more than 10 μ s¹⁸⁰ and to support magnon propagation over distances exceeding 100 μ m using a 110 nm-thin YIG liquid-phase epitaxy (LPE) film.¹⁸¹

For advanced quantum magnonic operations, longer magnon lifetimes are required. Previous experiments used the Kittel mode, a uniform precession of the magnetization across the whole sample. The damping of the FMR mode and dipolar magnons with large wavelengths is dominated by two-magnon scattering from lattice and surface defects, and is therefore largely temperature independent. On cooling to millikelvin temperatures, the lifetime decreases only slightly compared with RT^{56,70,73}. In contrast, short-wavelength magnons with finite wave vector, that are localized inside the sample, are insensitive to surface quality. For these dipolar-exchange spin waves (DESW) the dominant dissipation is scattering from thermal magnons and phonons. Recently, Serha *et al.*⁵⁶ showed that when this thermal bath is depleted the lifetime of short-wavelength magnons increases by more than an order of magnitude and reaches up to 18 μ s. These magnons were generated through the intrinsic nonlinearity of the system via three-magnon splitting, with the lifetime set by the power threshold for entering the nonlinear regime¹⁸².

The lifetime of these secondary magnons increases drastically as the temperature decreases from a few kelvin to the millikelvin range, as shown in Fig. 1 (f). As the temperature approaches absolute zero, multimagnon scattering on

thermal magnons and interactions with thermal phonons vanish, and because short-wavelength DESW remain localized within the crystal volume and are effectively decoupled from dipolar coupling to surrounding dissipation channels, their intrinsic relaxation is strongly suppressed, resulting in a pronounced enhancement of the magnon lifetime at millikelvin temperatures⁵⁶.

In theory, the lifetime of these magnons is expected to approach infinity at millikelvin temperatures. In practice, however, it saturates below about 250 mK⁵⁶. Interestingly, this saturation occurs at different lifetime levels, with crystal contamination with rare and heavy metal ions becoming the limiting factor. This impurity-induced lifetime-limiting bottleneck is evident in Fig. 1 (f), where a reduction in impurity concentration from Sphere 1 to Sphere 3 leads to an increase in the saturation lifetime of DESW magnons from approximately 5 μ s to 18 μ s. As higher-purity samples exhibit longer magnon lifetimes, indicating that values beyond 20 μ s — the dephasing time T_2 of state-of-the-art superconducting qubits¹⁸³ — are within reach when YIG is grown from specially purified yttrium oxide (Y_2O_3), which contains most of the rare-earth and L -state transition metal ion responsible for limiting YIG quality at low temperatures.

In total, DESW exhibit lifetimes at millikelvin temperatures that are long enough to transport quantum information and entanglement in micrometer- and submicrometer-thick films, for example between superconducting qubits. This paves the way for new experiments and applications in quantum magnonics, where magnons act as efficient carriers of quantum information.

III. YIG FILMS FOR QUANTUM MAGNONICS

To use magnons as quantum data carriers in quantum magnonics, it is crucial to move beyond standing magnons in spherical resonators^{4,6,33,48,188} and establish YIG films as the active medium for propagating single magnons. At RT, the highest bulk-like quality YIG films, from micrometer to nanometer scales, have been grown on paramagnetic GGG substrates because of the nearly perfect lattice matching between the two crystals^{189–196}.

However, quantum magnonics must operate at very low temperatures down to the millikelvin range. Under these conditions, paramagnetic substrates, such as GGG become readily magnetized by an externally applied magnetic field^{66,197}. Counterintuitively, the GGG substrate does not behave as a simple paramagnet describable by a Brillouin function at temperatures below 500 mK. Instead, in this temperature range it exhibits a complex magnetic phase diagram and enters a frustrated magnetic state, in which the magnetization becomes nearly temperature independent and is governed primarily by the external magnetic field^{66,198–200}. The magnetized substrate generates an inhomogeneous stray field that depends on its geometry and imposes a strong gradient in the internal field of the YIG film. For example, a common ($5 \times 5 \times 0.5$) mm³ GGG substrate at 1.8 K and an in-plane bias field of 600 mT produces stray fields of up to 60 mT at

TABLE II. Comparison of bulk YIG and thin YIG films relevant to quantum magnonics.

Property	bulk YIG ^{56,81,83}	YIG/GGG ⁷²	YIG/YSGG ¹⁸⁴	YIG/YSGAG ⁷²
Saturation magnetization M_s @ RT \rightarrow 0 K (kA/m)	140 200	144 205	67 95	131 184
Gilbert damping α @ RT ($\times 10^{-5}$)	3 ± 0.5	4.3 ± 0.4	10 ± 1	4.3 ± 0.6
Inhomogeneous linewidth broadening ΔB_0 @ RT (mT)	0 – 0.05	0.14	0.50	0.15
FMR linewidth ΔB @ \approx 8 GHz @ RT \rightarrow 0 K (mT)	0.03 0.02	0.19 0.85	0.50 0.75	0.17 0.25

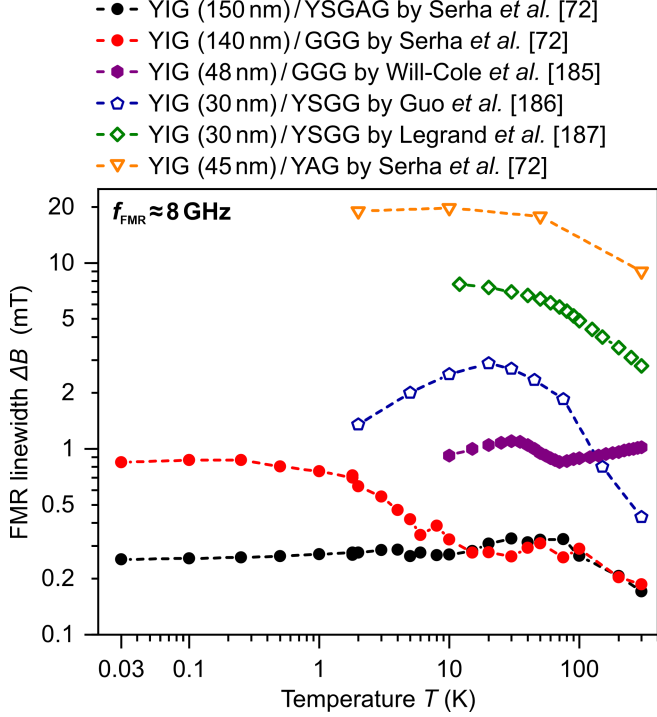


FIG. 2. FMR FWHM linewidth ΔB (measure for magnetic damping) as a function of temperature T for an FMR frequency $f_{\text{FMR}} \approx 8$ GHz, displayed on a double logarithmic scale. The graph compares measurements obtained in this work with selected results of sputtered (hollow symbols) and LPE grown (filled symbols) YIG films from relevant literature, enabling a direct evaluation of temperature-dependent damping behavior across different samples, their substrates and studies^{72,185–187}. Reproduced from R. O. Serha *et al.*, arXiv:2508.19044 (2025); licensed under a Creative Commons Attribution-NonCommercial-NoDerivatives 4.0 International (CC BY-NC-ND) license.

the edges and about 12 mT at the center opposing the external field⁶⁶. This gradient is already broadening the FMR linewidths measured over the sample⁶⁵. By selecting an appropriate substrate geometry or by microstructuring the YIG film, the GGG-induced stray-field gradient can be eliminated across the magnetic medium, resulting in a homogeneous internal field in YIG²⁰¹. However, the partially magnetically ordered substrate couples to the YIG spin system⁷³, opening extra dissipation channels that broaden the ferromagnetic resonance (FMR) linewidth^{65–70} and reduce magnon lifetimes of propagating dipolar magnons⁷³. The linewidth broadening effect is shown in Fig. 1 (g)⁶⁵ and Tab. II reports a linewidth

difference of more than a factor of four between RT and $T \rightarrow 0$, even in the absence of the inhomogeneous GGG-induced stray field. Such a decrease in magnon lifetime undermines the advantages that YIG would otherwise offer for quantum-magnonic experiments. Microstructuring²⁰¹ and operating at low external fields⁶⁴ can mitigate the stray-field gradient to some extent. Nevertheless, eliminating the coupling between the substrate spin system and the YIG film requires the use of diamagnetic substrates. For a comparison of the temperature-dependent damping behavior between YIG films grown on GGG and on diamagnetic alternative substrates, Fig. 2 presents literature results on sputtered and LPE-grown YIG films from different studies^{72,185–187}.

Yttrium aluminum garnet (YAG) was among the first diamagnetic substrates proposed to replace paramagnetic GGG in YIG heterostructures, aiming to unlock new possibilities for quantum magnonics at cryogenic temperatures by avoiding substrate magnetization in applied fields. However, despite the drawbacks of GGG at low temperatures, YIG/GGG still outperforms YIG/YAG at both RT and low temperature (see Fig. 2), primarily because the large lattice mismatch between YIG and YAG degrades crystalline quality of the YIG film^{72,202,203}.

In general, the broad garnet family^{204,205} offers promising diamagnetic substrates with lattice constants closely matching YIG. For example, yttrium scandium aluminum garnet (YSAG), used as a diamagnetic spacer between YIG and GGG, has been shown to reduce damping in YIG films at low temperatures⁶⁷. A stronger candidate is yttrium scandium gallium garnet (YSGG), which can serve directly as a substrate^{186,187}. YIG/YSGG has caught up with YIG/GGG in terms of FMR linewidth at low temperatures¹⁸⁴ (see Tab. II), and even demonstrated robust and superior spin-wave propagation at 2 K²⁰⁶. However, this improvement comes at the cost of lower saturation magnetization, which yields slower dipolar magnons, as the group velocity of magnetostatical spin waves are practically directly proportional to the magnetization saturation. In addition, for YIG/YSGG, only thin films of about 60 nm can be grown fully strained due to the large lattice mismatch, and these still do not reach the best room-temperature damping values achieved by YIG grown on GGG substrates⁷².

A breakthrough in the field came with the introduction of yttrium scandium gallium aluminum garnet (YSGAG) by C. Gugushev and C. Dubs *et al.*⁷¹. This diamagnetic garnet enables improved lattice matching up to no mismatch with YIG. Figure 1 (h) illustrates the $\text{Y}_3(\text{Sc}, \text{Ga}, \text{Al})_2(\text{Ga}, \text{Al})_3\text{O}_{12}$ crystal structure, highlighting selected dodecahedral, octahe-

dral, and tetrahedral oxygen coordination polyhedra with the corresponding ions at their centers. By customizing the distribution ratio of the diamagnetic ions Sc, Ga, and Al on the octahedral and tetrahedral sites, the lattice parameter can be tuned to match that of epitaxial YIG films⁷¹. As shown in Fig. 2, taken from the study⁷², YIG films grown by LPE on YSGAG exhibit simultaneously the same low damping at RT and at millikelvin temperatures that YIG on GGG achieves only at RT, thereby eliminating the drawbacks at cryogenic temperatures associated with paramagnetic substrates. Using YSGAG as the substrate, record-low FMR damping in YIG films were observed also at RT, with FMR linewidths as narrow as 0.1 mT at frequencies up to 4 GHz and a Gilbert damping parameter $\alpha = 4.29 \times 10^{-5}$.

From the properties summarized in Tab. II, it is clear that the YIG/YSAG system comes closest to bulk YIG at cryogenic temperatures. Its magnon lifetime is still shorter by a factor of about 5–10 compared with ultra-pure bulk YIG⁵⁶. However, YIG LPE film quality is known to improve with increasing thicknesses¹⁸⁹, and careful co-tuning of the YIG and YSGAG lattice parameters can yield an essentially perfect match of both systems. This approach enables YIG films with bulk-like magnetic quality at millikelvin temperatures—an ideal platform for studying single-magnon propagation in quantum magnonics.

IV. OUTLOOK

Quantum magnonics is inherently materials-driven, with ongoing efforts focused on identifying magnetic systems whose properties best match the demands of coherence, frequency, coupling strength, and scalability for a given application. Ferromagnetic metals and Heusler compounds offer large saturation magnetization, strong exchange, and excellent compatibility with nanofabrication, enabling strong coupling to microwave photons, spin currents, and superconducting circuits, but their finite electrical conductivity introduces intrinsic dissipation that presently limits magnon lifetimes to the nanosecond regime. Organic magnets provide chemically and structurally tunable systems and have demonstrated comparatively long lifetimes for their class, reaching tens of nanoseconds, yet remain constrained by disorder, interfacial effects, and the lack of systematic investigations at millikelvin temperatures. Magnetic insulators with high magnetization saturation or anisotropy, such as hexaferrites and europium chalcogenides, open access to high-frequency magnon modes and large magnon energies, offering prospects for bias-field-free operation in waveguides and high-frequency quantum magnonics, although challenges in thin-film growth, and low-temperature damping must still be addressed. Taken together, these diverse material classes highlight that future progress in quantum magnonics will rely on targeted materials optimization across multiple platforms rather than on a single universal material system.

Within this diverse materials landscape, two converging breakthroughs are leading to the perspective using ultra-long-living propagating magnons for future solid-state quantum

technologies. First, diamagnetic YSGAG substrates with a compositionally tunable lattice can be matched to YIG for nanometer-thin as well as micrometer-thick films. This approach removes substrate magnetization and stray-field gradients at cryogenic temperatures, while preserving the room-temperature damping performance that has made YIG/GGG films the benchmark. Second, in ultra pure YIG up to 18 μ s microsecond lifetimes for short wavelength dipolar-exchange magnons were demonstrated once the thermal magnon bath is depleted, showing that long coherence is available when impurities and extrinsic scattering are suppressed. Together, these results point to YIG films that support single magnon excitation, their propagation, and manipulation on-chip opening new directions for solid-state quantum magnonics.

A practical route to this goal is already provided by nanometer-thin YIG films grown on YSGAG. For submicrometer- or micrometer-thick films, an even better lattice match between the substrate and YIG is required. Such a perfectly matched, diamagnetic system would avoid the cryogenic drawbacks of paramagnetic GGG or strained substrate/YIG combinations, allowing the film to approach the intrinsic low dissipation of bulk YIG. In this regime, magnon lifetimes are governed mainly by material imperfections, making growth and processing critical: impurity levels must approach ultra-pure single-crystal quality with strict control of rare-earth contamination, while careful surface and edge preparation suppresses two-magnon scattering. At millikelvin temperatures, dipolar-exchange magnons reach lifetimes above ten microseconds. A remaining obstacle is that DESWs achieve long lifetimes by being insensitive to surfaces, but this also implies the low group velocity of dipolar waves, and their lifetime is expected to decrease with the increase in velocity. One potential solution would be to use low-frequency exchange waves with wavelengths shorter than the DESW, with reduced two-magnon scattering efficiencies and high group velocities.

Taken together, these elements will provide access to long-living and long-propagating single magnons that can be used as magnonic quantum information carriers. These carriers can serve as entanglement busses or gates between superconducting qubits placed on the same YSGAG substrates. Consequently, such single magnons will enable the integration of ‘classical magnonics’ data processing approaches, including RF applications, Boolean and neuromorphic computing, with magnon-based quantum computing concepts on the same nanoscale chip.

ACKNOWLEDGMENTS

This research was funded in part by the Austrian Science Fund (FWF) project Paramagnonics [10.55776/I6568]. The work was supported by the German Federal Ministry of Research, Technology and Space (BMFTR) under the reference numbers (13N17109) within a collaborative project “Low-loss materials for integrated magnonic-superconducting quantum technologies (MagSQuant)”. The authors thank Khrystyna O. Levchenko for insightful consultations and valuable scientific

discussions on magnetic materials, in particular on hexaferrites.

DATA AVAILABILITY STATEMENT

Data sharing is not applicable to this article as no new data were created or analyzed in this study.

- ¹M. A. Nielsen and I. L. Chuang, *Quantum Computation and Quantum Information*, 10th ed. (Cambridge University Press, Cambridge, UK, 2010).
- ²F. Arute, K. Arya, R. Babbush, D. Bacon, J. C. Bardin, R. Barends, R. Biswas, S. Boixo, F. G. S. L. Brandao, D. A. Buell, B. Burkett, Y. Chen, Z. Chen, B. Chiaro, R. Collins, W. Courtney, A. Dunsworth, E. Farhi, B. Foxen, A. Fowler, C. Gidney, M. Giustina, R. Graff, K. Guerin, S. Habegger, M. P. Harrigan, M. J. Hartmann, A. Ho, M. Hoffmann, T. Huang, T. S. Humble, S. V. Isakov, E. Jeffrey, Z. Jiang, D. Kafri, K. Kechedzhi, J. Kelly, P. V. Klimov, S. Knysh, A. Korotkov, F. Kostritsa, D. Landhuis, M. Lindmark, E. Lucero, D. Lyakh, S. Mandrà, J. R. McClean, M. McEwen, A. Megrant, X. Mi, K. Michielsen, M. Mohseni, J. Mutus, O. Naaman, M. Neeley, C. Neill, M. Y. Niu, E. Ostby, A. Petukhov, J. C. Platt, C. Quintana, E. G. Rieffel, P. Roushan, N. C. Rubin, D. Sank, K. J. Satzinger, V. Smelyanskiy, K. J. Sung, M. D. Trevithick, A. Vainsencher, B. Villalonga, T. White, Z. J. Yao, P. Yeh, A. Zalcman, H. Neven, and J. M. Martinis, “Quantum supremacy using a programmable superconducting processor,” *Nature* **574**, 505–510 (2019).
- ³A. V. Chumak, P. Kabos, M. Wu, C. Abert, C. Adelmann, A. O. Adeyeye, J. Åkerman, F. G. Aliev, A. Anane, A. Awad, C. H. Back, A. Barmann, G. E. W. Bauer, M. Becherer, E. N. Beginin, V. A. S. V. Bittencourt, Y. M. Blanter, P. Bortolotti, I. Boventer, D. A. Bozhko, S. A. Bunyayev, J. J. Carmiggelt, R. R. Cheenikundil, F. Ciubotaru, S. Cotofana, G. Csaba, O. V. Dobrovolskiy, C. Dubs, M. Elyasi, K. G. Fripp, H. Fulara, I. A. Golovchanskiy, C. Gonzalez-Ballester, P. Graczyk, D. Grundler, P. Gruszecki, G. Gubbiotti, K. Guslienko, A. Haldar, S. Hamdioui, R. Hertel, B. Hillebrands, T. Hioki, A. Houshang, C.-M. Hu, H. Huebl, M. Huth, E. Iacocca, M. B. Jungfleisch, G. N. Kakazei, A. Khitun, R. Khymyn, T. Kikkawa, M. Kläui, O. Klein, J. W. Klos, S. Knauer, S. Koraltan, M. Kostylev, M. Krawczyk, I. N. Krivorotov, V. V. Kruglyak, D. Lachance-Quirion, S. Ladak, R. Lebrun, Y. Li, M. Lindner, R. Macêdo, S. Mayr, G. A. Melkov, S. Mieszczak, Y. Nakamura, H. T. Nembach, A. A. Nikitin, S. A. Nikitov, V. Novosad, J. A. Otálora, Y. Otani, A. Papp, B. Pigeau, P. Pirro, W. Porod, F. Porrati, H. Qin, B. Rana, T. Reimann, F. Riente, O. Romero-Isart, A. Ross, A. V. Sadovnikov, A. R. Safin, E. Saitoh, G. Schmidt, H. Schultheiss, K. Schultheiss, A. A. Serga, S. Sharma, J. M. Shaw, D. Suess, O. Surzhenko, K. Szulc, T. Taniguchi, M. Urbánek, K. Usami, A. B. Ustinov, T. van der Sar, S. van Dijken, V. I. Vasyuchka, R. Verba, S. V. Kusminskiy, Q. Wang, M. Weides, M. Weiler, S. Wintz, S. P. Wolski, and X. Zhang, “Advances in magnetism roadmap on spin-wave computing,” *IEEE Transactions on Magnetics* **58**, 1–72 (2022).
- ⁴D. Lachance-Quirion, Y. Tabuchi, A. Gloppe, K. Usami, and Y. Nakamura, “Hybrid quantum systems based on magnonics,” *Applied Physics Express* **12**, 070101 (2019).
- ⁵Y. Li, W. Zhang, V. Tyberkevych, W. K. Kwok, A. Hoffmann, and V. Novosad, “Hybrid magnonics: Physics, circuits, and applications for coherent information processing,” *J. Appl. Phys.* **128**, 130902 (2020).
- ⁶Y. Li, V. G. Yefremenko, M. Lisovenko, C. Trevillian, T. Polakovic, T. W. Cecil, P. S. Barry, J. Pearson, R. Divan, V. Tyberkevych, C. L. Chang, U. Welp, W.-K. Kwok, and V. Novosad, “Coherent coupling of two remote magnonic resonators mediated by superconducting circuits,” *Physical Review Letters* **128** (2022), 10.1103/physrevlett.128.047701.
- ⁷H. Yuan, Y. Cao, A. Kamra, R. A. Duine, and P. Yan, “Quantum magnonics: When magnon spintronics meets quantum information science,” *Physics Reports* **965**, 1–74 (2022).
- ⁸X. Zhang, “A review of common materials for hybrid quantum magnonics,” *Materials Today Electronics* **5**, 100044 (2023).
- ⁹K. O. Levchenko, K. Davidková, J. Mikkelsen, and A. V. Chumak, “Review on spin-wave RF applications,” *IEEE Transactions on Magnetics* , 1–1 (2026).
- ¹⁰Q. Wang, B. Heinz, R. Verba, M. Kewenig, P. Pirro, M. Schneider, T. Meyer, B. Lägél, C. Dubs, T. Brächer, and A. Chumak, “Spin pinning and spin-wave dispersion in nanoscopic ferromagnetic waveguides,” *Physical Review Letters* **122** (2019), 10.1103/physrevlett.122.247202.
- ¹¹B. Heinz, T. Brächer, M. Schneider, Q. Wang, B. Lägél, A. M. Friedel, D. Breitbach, S. Steinert, T. Meyer, M. Kewenig, C. Dubs, P. Pirro, and A. V. Chumak, “Propagation of spin-wave packets in individual nanosized yttrium iron garnet magnonic conduits,” *Nano Letters* **20**, 4220–4227 (2020), arXiv:1910.08801.
- ¹²A. V. Chumak, A. A. Serga, and B. Hillebrands, “Magnonic crystals for data processing,” *Journal of Physics D: Applied Physics* **50**, 244001 (2017).
- ¹³A. V. Chumak, A. A. Serga, and B. Hillebrands, “Magnon transistor for all-magnon data processing,” *Nature Communications* **5**, 4700 (2014).
- ¹⁴Q. Wang, G. Csaba, R. Verba, A. V. Chumak, and P. Pirro, “Nanoscale magnonic networks,” *Physical Review Applied* **21** (2024), 10.1103/physrevapplied.21.040503.
- ¹⁵P. Pirro, V. I. Vasyuchka, A. A. Serga, and B. Hillebrands, “Advances in coherent magnonics,” *Nature Reviews Materials* **6**, 1114–1135 (2021).
- ¹⁶Q. Wang, R. Verba, B. Heinz, M. Schneider, O. Wojewoda, K. Davidková, K. Levchenko, C. Dubs, N. J. Mauser, M. Urbánek, P. Pirro, and A. V. Chumak, “Deeply nonlinear excitation of self-normalized short spin waves,” *Science Advances* **9** (2023), 10.1126/sciadv.adg4609.
- ¹⁷N. Zenbaa, K. O. Levchenko, J. Panda, K. Davidková, M. Ruhwedel, S. Knauer, M. Lindner, C. Dubs, Q. Wang, M. Urbánek, P. Pirro, and A. V. Chumak, “YIG/CoFeB bilayer magnonic isolator,” *IEEE Magnetics Letters* **16**, 1–5 (2025).
- ¹⁸S. O. Demokritov, V. E. Demidov, O. Dzyapko, G. A. Melkov, A. A. Serga, B. Hillebrands, and A. N. Slavin, “Bose–Einstein condensation of quasi-equilibrium magnons at room temperature under pumping,” *Nature* **443**, 430 (2006).
- ¹⁹A. A. Serga, V. S. Tiberkevich, C. W. Sandweg, V. I. Vasyuchka, D. A. Bozhko, A. V. Chumak, T. Neumann, B. Orby, G. A. Melkov, A. N. Slavin, and B. Hillebrands, “Bose–Einstein condensation in an ultra-hot gas of pumped magnons,” *Nature Communications* **5**, 3452 (2014).
- ²⁰M. Schneider, T. Brächer, D. Breitbach, V. Lauer, P. Pirro, D. A. Bozhko, M.-S. H. Y., B. Heinz, Q. Wang, T. Meyer, F. Heussner, S. Keller, E. T. Papaionnou, B. Lägél, T. Löber, C. Dubs, A. N. Slavin, V. S. Tiberkevich, A. A. Serga, B. Hillebrands, and A. V. Chumak, “Bose–Einstein condensation of quasiparticles by rapid cooling,” *Nature Nanotechnology* **15**, 457 (2020).
- ²¹M. Schneider, D. Breitbach, R. O. Serha, Q. Wang, M. Mohseni, A. A. Serga, A. N. Slavin, V. S. Tiberkevich, B. Heinz, T. Brächer, B. Lägél, C. Dubs, S. Knauer, O. V. Dobrovolskiy, P. Pirro, B. Hillebrands, and A. V. Chumak, “Stabilization of a nonlinear magnonic bullet coexisting with a Bose–Einstein condensate in a rapidly cooled magnonic system driven by spin-orbit torque,” *Physical Review B* **104**, L140405 (2021).
- ²²D. A. Bozhko, A. A. Serga, P. Clausen, V. V. Vasyuchka, F. Heussner, G. A. Melkov, A. Pomyalov, V. S. L’vov, and B. Hillebrands, “Supercurrent in a room-temperature Bose–Einstein magnon condensate,” *Nature Physics* **12**, 1057 (2016).
- ²³A. J. Kreil, D. A. Bozhko, H. Y. Musiienko-Shmarova, V. I. Vasyuchka, V. S. L’vov, A. Pomyalov, B. Hillebrands, and A. A. Serga, “From kinetic instability to Bose–Einstein condensation and magnon supercurrents,” *Physical Review Letters* **121** (2018), 10.1103/physrevlett.121.077203.
- ²⁴R. O. Serha, V. I. Vasyuchka, A. A. Serga, and B. Hillebrands, “Towards an experimental proof of the magnonic Aharonov–Casher effect,” *Physical Review B* **108**, L220404 (2023).
- ²⁵K. Nakata, K. A. van Hoogdalem, P. Simon, and D. Loss, “Josephson and persistent spin currents in Bose–Einstein condensates of magnons,” *Physical Review B* **90**, 144419 (2014).
- ²⁶I. Boventer, H. T. Simensen, B. Brekke, M. Weides, A. Anane, M. Kläui, A. Brataas, and R. Lebrun, “Antiferromagnetic cavity magnon polaritons in collinear and canted phases of hematite,” *Physical Review Applied* **19** (2023), 10.1103/physrevapplied.19.014071.
- ²⁷T. E. Kritzell, A. Baydin, F. Tay, R. Rodriguez, J. Doumani, H. Nojiri, H. O. Everitt, I. Barsukov, and J. Kono, “Terahertz cavity magnon polaritons,” *Advanced Optical Materials* **12** (2023), 10.1002/adom.202302270.
- ²⁸H. Wang, R. Yuan, Y. Zhou, Y. Zhang, J. Chen, S. Liu, H. Jia, D. Yu, J.-P. Ansermet, C. Song, and H. Yu, “Long-distance coherent propagation of

- high-velocity antiferromagnetic spin waves,” *Physical Review Letters* **130**, 096701 (2023).
- ²⁹A. G. Gurevich and G. A. Melkov, “Magnetization oscillations and waves,” (CRC Press, 1996) pp. 74–75, 1st ed.
- ³⁰A. A. Clerk, M. H. Devoret, S. M. Girvin, F. Marquardt, and R. J. Schoelkopf, “Introduction to quantum noise, measurement, and amplification,” *Reviews of Modern Physics* **82**, 1155–1208 (2010).
- ³¹Y. Tabuchi, S. Ishino, A. Noguchi, T. Ishikawa, R. Yamazaki, K. Usami, and Y. Nakamura, “Coherent coupling between a ferromagnetic magnon and a superconducting qubit,” *Science* **349**, 405–408 (2015).
- ³²S. P. Wolski, D. Lachance-Quirion, Y. Tabuchi, S. Kono, A. Noguchi, K. Usami, and Y. Nakamura, “Dissipation-based quantum sensing of magnons with a superconducting qubit,” *Physical Review Letters* **125**, 117701 (2020).
- ³³D. Lachance-Quirion, S. P. Wolski, Y. Tabuchi, S. Kono, K. Usami, and Y. Nakamura, “Entanglement-based single-shot detection of a single magnon with a superconducting qubit,” *Science* **367**, 425–428 (2020).
- ³⁴P. G. Baity, D. A. Bozhko, R. Macêdo, W. Smith, R. C. Holland, S. Danilin, V. Seferai, J. Barbosa, R. R. Peroor, S. Goldman, U. Nasti, J. Paul, R. H. Hadfield, S. McVitie, and M. Weides, “Strong magnon–photon coupling with chip-integrated yig in the zero-temperature limit,” *Applied Physics Letters* **119**, 033502 (2021).
- ³⁵X. Zuo, Z.-Y. Fan, H. Qian, M.-S. Ding, H. Tan, H. Xiong, and J. Li, “Cavity magnomechanics: from classical to quantum,” *New Journal of Physics* **26**, 031201 (2024).
- ³⁶M. Kounalakis, G. E. W. Bauer, and Y. M. Blanter, “Analog quantum control of magnonic cat states on a chip by a superconducting qubit,” *Physical Review Letters* **129** (2022), 10.1103/physrevlett.129.037205.
- ³⁷Z. Jiang, J. Lim, Y. Li, W. Pfaff, T.-H. Lo, J. Qian, A. Schleife, J.-M. Zuo, V. Novosad, and A. Hoffmann, “Integrating magnons for quantum information,” *Applied Physics Letters* **123** (2023), 10.1063/5.0157520.
- ³⁸M. Dols, S. Sharma, L. Bechara, Y. M. Blanter, M. Kounalakis, and S. Viola Kusminskiy, “Magnon-mediated quantum gates for superconducting qubits,” *Physical Review B* **110** (2024), 10.1103/physrevb.110.104416.
- ³⁹S. Dey, G. Rivero-Carracedo, A. Shumilin, C. Gonzalez-Ballester, and J. J. Baldoví, “Coupling molecular spin qubits with 2D magnets for coherent magnon manipulation,” *Nano Letters* **25**, 10457–10464 (2025).
- ⁴⁰M. Kostylev, A. B. Ustinov, A. V. Drozdovskii, B. A. Kalinikos, and E. Ivanov, “Towards experimental observation of parametrically squeezed states of microwave magnons in yttrium iron garnet films,” *Physical Review B* **100**, 020401 (2019).
- ⁴¹Z.-B. Yang, H. Jin, J.-W. Jin, J.-Y. Liu, H.-Y. Liu, and R.-C. Yang, “Bistability of squeezing and entanglement in cavity magnonics,” *Physical Review Research* **3** (2021), 10.1103/physrevresearch.3.023126.
- ⁴²Z. Haghshenasfard and M. G. Cottam, “Sub-poissonian statistics and squeezing of magnons due to the kerr effect in a hybrid coupled cavity–magnon system,” *Journal of Applied Physics* **128**, 033901 (2020).
- ⁴³Z. Toklikishvili, L. Chotorlishvili, R. Khomeriki, V. Jandieri, and J. Berakdar, “Electrically controlled entanglement of cavity photons with electromagnons,” *Physical Review B* **107** (2023), 10.1103/physrevb.107.115126.
- ⁴⁴S. Sharma, S. Viola Kusminskiy, and V. A. S. V. Bittencourt, “Quantum tomography of magnons using brillouin light scattering,” *Physical Review B* **110** (2024), 10.1103/physrevb.110.014416.
- ⁴⁵T.-X. Lu, X. Xiao, L.-S. Chen, Q. Zhang, and H. Jing, “Magnon-squeezing-enhanced slow light and second-order sideband in cavity magnomechanics,” *Physical Review A* **107** (2023), 10.1103/physreva.107.063714.
- ⁴⁶Q. Zhang, Y. Zhou, F. Liu, X. Wang, Y. Gao, L. Fan, and C. Cao, “Magnon-squeezing-enhanced phonon lasing in cavity magnomechanics,” *Advanced Quantum Technologies* (2024), 10.1002/ajte.202400200.
- ⁴⁷M. Song, T. Polakovic, J. Lim, T. W. Cecil, J. Pearson, R. Divan, W.-K. Kwok, U. Welp, A. Hoffmann, K.-J. Kim, V. Novosad, and Y. Li, “Single-shot magnon interference in a magnon-superconducting-resonator hybrid circuit,” *Nature Communications* **16** (2025), 10.1038/s41467-025-58482-2.
- ⁴⁸D. Xu, X.-K. Gu, H.-K. Li, Y.-C. Weng, Y.-P. Wang, J. Li, H. Wang, S.-Y. Zhu, and J. You, “Quantum control of a single magnon in a macroscopic spin system,” *Phys. Rev. Lett.* **130**, 193603 (2023).
- ⁴⁹D. Xu, X.-K. Gu, Y.-C. Weng, H.-K. Li, Y.-P. Wang, S.-Y. Zhu, and J. Q. You, “Macroscopic bell state between a millimeter-sized spin system and a superconducting qubit,” *Quantum Science and Technology* **9**, 035002 (2024).
- ⁵⁰M. Fukami, J. C. Marcks, D. R. Candido, L. R. Weiss, B. Soloway, S. E. Sullivan, N. Deegan, F. J. Heremans, M. E. Flatté, and D. D. Awschalom, “Magnon-qubit coupling determined via dissipation measurements,” *Proceedings of the National Academy of Sciences* **121** (2024), 10.1073/pnas.2313754120.
- ⁵¹M. Borst, P. H. Vree, A. Lowther, A. Teepe, S. Kurdi, I. Bertelli, B. G. Simon, Y. M. Blanter, and T. van der Sar, “Observation and control of hybrid spin-wave–meissner-current transport modes,” *Science* **382**, 430–434 (2023).
- ⁵²P. Krantz, M. Kjaergaard, F. Yan, T. P. Orlando, S. Gustavsson, and W. D. Oliver, “A quantum engineer’s guide to superconducting qubits,” *Applied Physics Reviews* **6**, 021318 (2019).
- ⁵³Z. Haghshenasfard and M. G. Cottam, “Quantum statistics and squeezing for a microwave-driven interacting magnon system,” *Journal of Physics: Condensed Matter* **29**, 045803 (2016).
- ⁵⁴M. E. Mycroft, R. O. Serha, A. V. Chumak, and C. Gonzalez-Ballester, “Quantum state preparation of ferromagnetic magnons by parametric driving,” arXiv:2601.12833 (2026), 10.48550/ARXIV.2601.12833.
- ⁵⁵A. A. Serga, A. V. Chumak, and B. Hillebrands, “YIG magnonics,” *Journal of Physics D: Applied Physics* **43**, 264002 (2010).
- ⁵⁶R. O. Serha, K. H. McAllister, F. Majcen, S. Knauer, T. Reimann, C. Dubs, G. A. Melkov, A. A. Serga, V. S. Tyberkevych, A. V. Chumak, and D. A. Bozhko, “Ultra-long-living magnons in the quantum limit,” arXiv:2505.22773 (2025), 10.48550/ARXIV.2505.22773.
- ⁵⁷M. Pita-Vidal, A. Bargerbos, C.-K. Yang, D. J. van Woerkom, W. Pfaff, N. Haider, P. Krogstrup, L. P. Kouwenhoven, G. de Lange, and A. Kou, “Gate-tunable field-compatible fluxonium,” *Physical Review Applied* **14**, 064038 (2020).
- ⁵⁸A. Kringhøj, T. W. Larsen, O. Erlandsson, W. Uilhoorn, J. Kroll, M. Hesselberg, R. McNeil, P. Krogstrup, L. Casparis, C. Marcus, and K. Petersson, “Magnetic-field-compatible superconducting transmon qubit,” *Physical Review Applied* **15**, 054001 (2021).
- ⁵⁹S. Günzler, J. Beck, D. Rieger, N. Gosling, N. Zapata, M. Field, S. Geisert, A. Bacher, J. K. Hohmann, M. Spiecker, W. Wernsdorfer, and I. M. Pop, “Spin environment of a superconducting qubit in high magnetic fields,” *Nature Communications* **16**, 9564 (2025).
- ⁶⁰K. O. Nikolaev, S. R. Lake, G. Schmidt, S. O. Demokritov, and V. E. Demidov, “Zero-field spin waves in yig nanowaveguides,” *Nano Letters* **23**, 8719–8724 (2023).
- ⁶¹R. O. Serha, A. Pomyalov, A. V. Chumak, and V. S. L’vov, “Unified theory of magnetization temperature dependence in ferrimagnets,” *Physical Review B* **112**, 174427 (2025).
- ⁶²A. Van Loo, R. Morris, and A. Karenowska, “Time-resolved measurements of surface spin-wave pulses at millikelvin temperatures,” *Physical Review Applied* **10**, 044070 (2018).
- ⁶³A. D. Karenowska, A. D. Patterson, M. J. Peterer, E. B. Magnússon, and P. J. Leek, “Excitation and detection of propagating spin waves at the single magnon level,” arXiv preprint arXiv:1502.06263 (2015).
- ⁶⁴S. Knauer, K. Davídková, D. Schmoll, R. O. Serha, A. Voronov, Q. Wang, R. Verba, O. V. Dobrovolskiy, M. Lindner, T. Reimann, *et al.*, “Propagating spin-wave spectroscopy in a liquid-phase epitaxial nanometer-thick YIG film at millikelvin temperatures,” *J. Appl. Phys.* **133**, 143905 (2023).
- ⁶⁵R. O. Serha, A. A. Voronov, D. Schmoll, R. Klingbeil, S. Knauer, S. Koraltan, E. Pribytova, M. Lindner, T. Reimann, C. Dubs, C. Abert, R. Verba, M. Urbánek, D. Suess, and A. V. Chumak, “Damping enhancement in YIG at millikelvin temperatures due to GGG substrate,” *Materials Today Quantum* **5**, 100025 (2025).
- ⁶⁶R. O. Serha, A. A. Voronov, D. Schmoll, R. Verba, K. O. Levchenko, S. Koraltan, K. Davídková, B. Budinská, Q. Wang, O. V. Dobrovolskiy, M. Urbánek, M. Lindner, T. Reimann, C. Dubs, C. Gonzalez-Ballester, C. Abert, D. Suess, D. A. Bozhko, S. Knauer, and A. V. Chumak, “Magnetic anisotropy and GGG substrate stray field in YIG films down to millikelvin temperatures,” *npj Spintronics* **2** (2024), 10.1038/s44306-024-00030-7.
- ⁶⁷S. Guo, B. McCullian, P. C. Hammel, and F. Yang, “Low damping at few-K temperatures in Y₃Fe₅O₁₂ epitaxial films isolated from Gd₃Ga₅O₁₂

- substrate using a diamagnetic $Y_3Sc_{2.5}Al_{2.5}O_{12}$ spacer,” *J. Magn. Magn. Mater.* **562**, 169795 (2022).
- ⁶⁸C. L. Jermain, S. V. Aradhya, N. D. Reynolds, R. A. Buhrman, J. T. Brangham, M. R. Page, P. C. Hammel, F. Y. Yang, and D. C. Ralph, “Increased low-temperature damping in yttrium iron garnet thin films,” *Physical Review B* **95**, 174411 (2017).
- ⁶⁹L. Mihalceanu, V. I. Vasyuchka, D. A. Bozhko, T. Langner, A. Y. Nechiporuk, V. F. Romanyuk, B. Hillebrands, and A. A. Serga, “Temperature-dependent relaxation of dipole-exchange magnons in yttrium iron garnet films,” *Physical Review B* **97**, 214405 (2018).
- ⁷⁰S. Kosen, A. F. van Loo, D. A. Bozhko, L. Mihalceanu, and A. D. Karenowska, “Microwave magnon damping in YIG films at millikelvin temperatures,” *APL Materials* **7**, 101120 (2019).
- ⁷¹C. Gugushev, C. Dubs, R. Blukis, O. Surzhenko, M. Brützmam, R. Koc, C. Rhode, K. Berger, C. Richter, C. Berryman, R. O. Serha, and A. V. Chumak, “Novel diamagnetic garnet-type substrate single crystals for ultralow-damping yttrium iron garnet $Y_3Fe_5O_{12}$ films at cryogenic temperatures,” arXiv:2508.18101 (2025), 10.48550/ARXIV.2508.18101.
- ⁷²R. O. Serha, C. Dubs, C. Gugushev, B. Aichner, D. Schmoll, J. Panda, M. Weiler, P. Pirro, M. Urbánek, and A. V. Chumak, “YSGAG: The ideal substrate for YIG in quantum magnonics,” arXiv:2508.19044 (2025), 10.48550/ARXIV.2508.19044.
- ⁷³D. Schmoll, A. A. Voronov, R. O. Serha, D. Slobodianiuk, K. O. Levchenko, C. Abert, S. Knauer, D. Suess, R. Verba, and A. V. Chumak, “Wavenumber-dependent magnetic losses in yttrium iron garnet-gadolinium gallium garnet heterostructures at millikelvin temperatures,” *Physical Review B* **111**, 134428 (2025).
- ⁷⁴A. Barman, G. Gubbiotti, S. Ladak, A. O. Adeyeye, M. Krawczyk, J. Grafe, C. Adelman, S. Cotofana, A. Naeemi, V. I. Vasyuchka, B. Hillebrands, S. A. Nikitov, H. Yu, D. Grundler, A. V. Sadovnikov, A. A. Grachev, S. E. Sheshukova, J. Y. Duquesne, M. Marangolo, G. Csaba, W. Porod, V. E. Demidov, S. Urazhdin, S. O. Demokritov, E. Albisetti, D. Petti, R. Bertacco, H. Schultheiss, V. V. Kruglyak, V. D. Poimanov, S. Sahoo, J. Sinha, H. Yang, M. Münzenberg, T. Moriyama, S. Mizukami, P. Landeros, R. A. Gallardo, G. Carlotti, J. V. Kim, R. L. Stamps, R. E. Camley, B. Rana, Y. Otani, W. Yu, T. Yu, G. E. Bauer, C. Back, G. S. Uhrig, O. V. Dobrovolskiy, B. Budinska, H. Qin, S. Van Dijken, A. V. Chumak, A. Khitun, D. E. Nikonov, I. A. Young, B. W. Zingsem, and M. Winklhofer, “The 2021 magnonics roadmap,” *Journal of Physics: Condensed Matter* **33**, 413001 (2021).
- ⁷⁵B. Flebus, D. Grundler, B. Rana, Y. Otani, I. Barsukov, A. Barman, G. Gubbiotti, P. Landeros, J. Akerman, U. Ebels, P. Pirro, V. E. Demidov, K. Schultheiss, G. Csaba, Q. Wang, F. Ciubotaru, D. E. Nikonov, P. Che, R. Hertel, T. Ono, D. Afanasiev, J. Mentink, T. Rasing, B. Hillebrands, S. V. Kusminskiy, W. Zhang, C. R. Du, A. Finco, T. van der Sar, Y. K. Luo, Y. Shiota, J. Sklenar, T. Yu, and J. Rao, “The 2024 magnonics roadmap,” *Journal of Physics: Condensed Matter* **36**, 363501 (2024).
- ⁷⁶A. V. Chumak, V. I. Vasyuchka, A. A. Serga, and B. Hillebrands, “Magnon spintronics,” *Nature Physics* **11**, 1505–1549 (2015).
- ⁷⁷M. Pardavi-Horvath, “Microwave applications of soft ferrites,” *Journal of Magnetism and Magnetic Materials* **215–216**, 171–183 (2000).
- ⁷⁸V. Cherepanov, I. Kolokolov, and V. L’vov, “The saga of YIG: Spectra, thermodynamics, interaction and relaxation of magnons in a complex magnet,” *Physics Reports* **229**, 81–144 (1993).
- ⁷⁹F. Bertaut and F. Forrat, “Structure of ferrimagnetic rare-earth ferrites,” *CR Acad. Sci* **242**, 382 (1956).
- ⁸⁰S. Geller and M. Gilleo, “The crystal structure and ferrimagnetism of yttrium-iron garnet, $Y_3Fe_2(FeO_4)_3$,” *Journal of Physics and Chemistry of Solids* **3**, 30–36 (1957).
- ⁸¹S. Klingler, H. Maier-Flaig, C. Dubs, O. Surzhenko, R. Gross, H. Huebl, S. T. B. Goennenwein, and M. Weiler, “Gilbert damping of magnetostatic modes in a yttrium iron garnet sphere,” *Applied Physics Letters* **110**, 092409 (2017).
- ⁸²S. Klingler, A. V. Chumak, T. Mewes, B. Khodadadi, C. Mewes, C. Dubs, O. Surzhenko, B. Hillebrands, and A. Conca, “Measurements of the exchange stiffness of YIG films using broadband ferromagnetic resonance techniques,” *Journal of Physics D: Applied Physics* **48**, 015001 (2014).
- ⁸³H. Maier-Flaig, S. Klingler, C. Dubs, O. Surzhenko, R. Gross, M. Weiler, H. Huebl, and S. T. B. Goennenwein, “Temperature-dependent magnetic damping of yttrium iron garnet spheres,” *Physical Review B* **95**, 214423 (2017).
- ⁸⁴V. E. Demidov and S. O. Demokritov, “Magnonic waveguides studied by microfocus brillouin light scattering,” *IEEE Transactions on Magnetism* **51**, 1–15 (2015).
- ⁸⁵S. S. Kalarickal, P. Krivosik, M. Wu, C. E. Patton, M. L. Schneider, P. Kabos, T. J. Silva, and J. P. Nibarger, “Ferromagnetic resonance linewidth in metallic thin films: Comparison of measurement methods,” *Journal of Applied Physics* **99** (2006), 10.1063/1.2197087.
- ⁸⁶T. Sebastian, K. Schultheiss, B. Obry, B. Hillebrands, and H. Schultheiss, “Micro-focused brillouin light scattering: imaging spin waves at the nanoscale,” *Frontiers in Physics* **3** (2015), 10.3389/fphy.2015.00035.
- ⁸⁷C. E. Patton, “Linewidth and relaxation processes for the main resonance in the spin-wave spectra of Ni-Fe alloy films,” *Journal of Applied Physics* **39**, 3060–3068 (1968).
- ⁸⁸A. Brunsch, “Magnetic properties and corrosion resistance of $(CoFeB)_{100-x}Cr_x$ thin films,” *Journal of Applied Physics* **50**, 7603–7605 (1979).
- ⁸⁹X. Liu, W. Zhang, M. J. Carter, and G. Xiao, “Ferromagnetic resonance and damping properties of CoFeB thin films as free layers in MgO-based magnetic tunnel junctions,” *Journal of Applied Physics* **110** (2011), 10.1063/1.3615961.
- ⁹⁰A. Conca, J. Greser, T. Sebastian, S. Klingler, B. Obry, B. Leven, and B. Hillebrands, “Low spin-wave damping in amorphous $Co_{40}Fe_{40}B_{20}$ thin films,” *Journal of Applied Physics* **113** (2013), 10.1063/1.4808462.
- ⁹¹J. Chen, Z. Jin, R. Yuan, H. Wang, H. Jia, W. Wei, L. Sheng, J. Wang, Y. Zhang, S. Liu, D. Yu, J.-P. Ansermet, P. Yan, and H. Yu, “Observation of coherent gapless magnons in an antiferromagnet,” *Physical Review Letters* **134** (2025), 10.1103/physrevlett.134.056701.
- ⁹²M. Hamdi, F. Posva, and D. Grundler, “Spin wave dispersion of ultralow damping hematite ($\alpha-Fe_2O_3$) at GHz frequencies,” *Physical Review Materials* **7** (2023), 10.1103/physrevmaterials.7.054407.
- ⁹³E. J. Samuelsen and G. Shirane, “Inelastic neutron scattering investigation of spin waves and magnetic interactions in $\alpha-Fe_2O_3$,” *physica status solidi (b)* **42**, 241–256 (1970).
- ⁹⁴Y.-Y. Song, Y. Sun, L. Lu, J. Bevivino, and M. Wu, “Self-biased planar millimeter wave notch filters based on magnetostatic wave excitation in barium hexagonal ferrite thin films,” *Applied Physics Letters* **97** (2010).
- ⁹⁵V. Harris, “Modern microwave ferrites,” *IEEE Transactions on Magnetism* **48** (2012), 10.1109/TMAG.2011.2180732.
- ⁹⁶L. Malkinski, “Advanced magnetic materials” (BoD–Books on Demand, 2012).
- ⁹⁷Q. Zhu, R. Tang, F. Peng, S. Xu, G. Liang, R. Zhao, Y. Fang, L. You, and X. Su, “Mechanical regulation of the magnetic properties of uniaxial anisotropic hexaferrite thin films,” *Physical Review Applied* **16**, 054006 (2021).
- ⁹⁸M. Popov, I. Zavislyak, H. Qu, A. Balbashov, M. Page, and G. Srinivasan, “In-plane current induced nonlinear magnetoelectric effects in single crystal films of barium hexaferrite,” *Scientific Reports* **12**, 5374 (2022).
- ⁹⁹C. Liu, C. K. A. Mewes, M. Chshiev, T. Mewes, and W. H. Butler, “Origin of low Gilbert damping in half metals,” *Applied Physics Letters* **95** (2009), 10.1063/1.3157267.
- ¹⁰⁰S. Trudel, O. Gaier, J. Hamrle, and B. Hillebrands, “Magnetic anisotropy, exchange and damping in cobalt-based full-heusler compounds: an experimental review,” *Journal of Physics D: Applied Physics* **43**, 193001 (2010).
- ¹⁰¹M. Oogane, T. Kubota, Y. Kota, S. Mizukami, H. Naganuma, A. Sakuma, and Y. Ando, “Gilbert magnetic damping constant of epitaxially grown cobased heusler alloy thin films,” *Applied Physics Letters* **96** (2010), 10.1063/1.3456378.
- ¹⁰²T. Sebastian, Y. Ohdaira, T. Kubota, P. Pirro, T. Brächer, K. Vogt, A. A. Serga, H. Naganuma, M. Oogane, Y. Ando, and B. Hillebrands, “Low-damping spin-wave propagation in a micro-structured $Co_2Mn_{0.6}Fe_{0.4}Si$ heusler waveguide,” *Applied Physics Letters* **100**, 112402 (2012).
- ¹⁰³D. K. de Wal, A. Iwens, T. Liu, P. Tang, G. E. W. Bauer, and B. J. van Wees, “Long-distance magnon transport in the van der waals antiferromagnet $CrPS_4$,” *Physical Review B* **107** (2023), 10.1103/physrevb.107.1180405.
- ¹⁰⁴S. L. Bud’ko, E. Gati, T. J. Slade, and P. C. Canfield, “Magnetic order in the van der waals antiferromagnet $CrPS_4$: Anisotropic $H-T$ phase diagrams and effects of pressure,” *Physical Review B* **103** (2021),

- 10.1103/physrevb.103.224407.
- ¹⁰⁵J. Lee, T. Y. Ko, J. H. Kim, H. Bark, B. Kang, S.-G. Jung, T. Park, Z. Lee, S. Ryu, and C. Lee, "Structural and optical properties of single- and few-layer magnetic semiconductor CrPS₄," *ACS Nano* **11**, 10935–10944 (2017).
 - ¹⁰⁶C. W. F. Freeman, H. Youel, A. K. Budniak, Z. Xue, H. De Libero, T. Thomson, M. Bosman, G. Eda, H. Kurebayashi, and M. Cubukcu, "Tunable ultrastrong magnon–magnon coupling approaching the deep-strong regime in a van der waals antiferromagnet," *ACS Nano* **19**, 16024–16031 (2025).
 - ¹⁰⁷O. Gomonay, V. Baltz, A. Brataas, and Y. Tserkovnyak, "Antiferromagnetic spin textures and dynamics," *Nature Physics* **14**, 213–216 (2018).
 - ¹⁰⁸A. Kamra, R. E. Troncoso, W. Belzig, and A. Brataas, "Gilbert damping phenomenology for two-sublattice magnets," *Physical Review B* **98**, 184402 (2018).
 - ¹⁰⁹H. T. Simensen, A. Kamra, R. E. Troncoso, and A. Brataas, "Magnon decay theory of gilbert damping in metallic antiferromagnets," *Physical Review B* **101**, 020403 (2020).
 - ¹¹⁰G. Talmelli, T. Devolder, N. Träger, J. Förster, S. Wintz, M. Weigand, H. Stoll, M. Heyns, G. Schütz, I. P. Radu, J. Gräfe, F. Ciubotaru, and C. Adelmann, "Reconfigurable submicrometer spin-wave majority gate with electrical transducers," *Sci. Adv.* **6** (2020), 10.1126/sciadv.abb4042.
 - ¹¹¹O. Wojewoda, J. Holobrádek, D. Pavelka, E. Pribytova, J. Krčma, J. Klíma, J. Panda, J. Michalička, T. Lednický, A. V. Chumak, and M. Urbánek, "Unidirectional propagation of zero-momentum magnons," *Applied Physics Letters* **125** (2024), 10.1063/5.0218478.
 - ¹¹²M. A. W. Schoen, D. Thonig, M. L. Schneider, T. J. Silva, H. T. Nembach, O. Eriksson, O. Karis, and J. M. Shaw, "Ultra-low magnetic damping of a metallic ferromagnet," *Nature Physics* **12**, 839–842 (2016).
 - ¹¹³O. Gladii, D. Halley, Y. Henry, and M. Bailleul, "Spin-wave propagation and spin-polarized electron transport in single-crystal iron films," *Physical Review B* **96**, 174420 (2017).
 - ¹¹⁴V. Korenman and R. E. Prange, "Anomalous damping of spin waves in magnetic metals," *Physical Review B* **6**, 2769–2777 (1972).
 - ¹¹⁵Y. Li, T. Polakovic, Y.-L. Wang, J. Xu, S. Lendinez, Z. Zhang, J. Ding, T. Khaire, H. Saglam, R. Divan, J. Pearson, W.-K. Kwok, Z. Xiao, V. Novosad, A. Hoffmann, and W. Zhang, "Strong coupling between magnons and microwave photons in on-chip ferromagnet-superconductor thin-film devices," *Physical Review Letters* **123**, 107701 (2019).
 - ¹¹⁶M. Naka, Y. Motome, and H. Seo, "Altermagnetic perovskites," *npj Spintronics* **3**, 1 (2025).
 - ¹¹⁷S. Mañas-Valero, T. van der Sar, R. A. Duine, and B. van Wees, "Fundamentals and applications of van der waals magnets in magnon spintronics," *Newton* **1**, 100018 (2025).
 - ¹¹⁸T. Graf, C. Felser, and S. S. Parkin, "Simple rules for the understanding of heusler compounds," *Progress in Solid State Chemistry* **39**, 1–50 (2011).
 - ¹¹⁹K. Elphick, W. Frost, M. Samiepour, T. Kubota, K. Takanashi, H. Sukegawa, S. Mitani, and A. Hirohata, "Heusler alloys for spintronic devices: review on recent development and future perspectives," *Science and Technology of Advanced Materials* **22**, 235–271 (2021).
 - ¹²⁰S. Manton, A. Torres Dias, M. Madami, S. Tacchi, and N. Biziere, "Reconfigurable spin wave modes in a heusler magnonic crystal," *Journal of Applied Physics* **135**, 053902 (2024).
 - ¹²¹C. Guillemard, S. Petit-Watlot, L. Pasquier, D. Pierre, J. Ghanbaja, J.-C. Rojas-Sánchez, A. Bataille, J. Rault, P. Le Fèvre, F. Bertran, and S. Andrieu, "Ultralow magnetic damping in Co₂Mn-based heusler compounds: Promising materials for spintronics," *Physical Review Applied* **11** (2019), 10.1103/physrevapplied.11.064009.
 - ¹²²A. V. Chumak, "Magnon spintronics," in *Spintronics Handbook: Spin Transport and Magnetism*, edited by E. Y. Tsymlal and I. Žutić (CRC Press, Boca Raton, FL, 2019) 2nd ed., pp. 247–302.
 - ¹²³O. M. Chumak, A. Pacewicz, A. Lynnyk, B. Salski, T. Yamamoto, T. Seki, J. Z. Domagala, H. Głowiński, K. Takanashi, L. T. Baczewski, H. Szymczak, and A. Napiórek, "Magnetoelastic interactions and magnetic damping in co2fe0.4mn0.6si and co2fega0.5ge0.5 heusler alloys thin films for spintronic applications," *Scientific Reports* **11**, 7608 (2021).
 - ¹²⁴C. J. Love, B. Kuerbanjiang, A. Kerrigan, S. Yamada, K. Hamaya, G. van der Laan, V. K. Lazarov, and S. A. Cavill, "Substrate dependent reduction of gilbert damping in annealed heusler alloy thin films grown on group iv semiconductors," *Applied Physics Letters* **119**, 172404 (2021).
 - ¹²⁵C. de Melo, C. Guillemard, A. Friedel, V. Palin, J. Rojas-Sánchez, S. Petit-Watlot, and S. Andrieu, "Unveiling transport properties of co2mnsi heusler epitaxial thin films with ultra-low magnetic damping," *Applied Materials Today* **25**, 101174 (2021).
 - ¹²⁶R. Wang, X. Chen, P. Yan, Y. Xu, Y. Zhang, J. Wang, R. Fan, P. Bencok, P. Steadman, Y. Li, W. Zou, Y. Xu, R. Liu, W. Liu, and L. He, "Modulation of the magnetization and gilbert damping in heusler-alloy co3–xfexal thin films," *Applied Physics Letters* **123**, 012403 (2023).
 - ¹²⁷S. Takei, B. I. Halperin, A. Yacoby, and Y. Tserkovnyak, "Superfluid spin transport through antiferromagnetic insulators," *Physical Review B* **90** (2014), 10.1103/physrevb.90.094408.
 - ¹²⁸V. Azimi-Mousolou, A. Bergman, A. Delin, O. Eriksson, M. Pereira, D. Thonig, and E. Sjöqvist, "Transmon probe for quantum characteristics of magnons in antiferromagnets," *Physical Review B* **108** (2023), 10.1103/physrevb.108.094430.
 - ¹²⁹A. Dyrdał, A. Qaiumzadeh, A. Brataas, and J. Barnaś, "Magnon-plasmon hybridization mediated by spin-orbit interaction in magnetic materials," *Physical Review B* **108** (2023), 10.1103/physrevb.108.045414.
 - ¹³⁰J. Gückelhorn, A. Kamra, T. Wimmer, M. Opel, S. Geprägs, R. Gross, H. Huebl, and M. Althammer, "Influence of low-energy magnons on magnon hangle experiments in easy-plane antiferromagnets," *Physical Review B* **105**, 094440 (2022).
 - ¹³¹A. El Kanj, O. Gomonay, I. Boverter, P. Bortolotti, V. Cros, A. Anane, and R. Lebrun, "Antiferromagnetic magnon spintronic based on nonreciprocal and nondegenerated ultra-fast spin-waves in the canted antiferromagnet α -Fe₂O₃," *Science Advances* **9** (2023), 10.1126/sciadv.adh1601.
 - ¹³²J. Gückelhorn, S. de-la Peña, M. Scheufele, M. Grammer, M. Opel, S. Geprägs, J. C. Cuevas, R. Gross, H. Huebl, A. Kamra, and M. Althammer, "Observation of the nonreciprocal magnon hangle effect," *Physical Review Letters* **130**, 216703 (2023).
 - ¹³³S. Das, A. Ross, X. X. Ma, S. Becker, C. Schmitt, F. van Duijn, E. F. Galindez-Ruales, F. Fuhrmann, M.-A. Syskaki, U. Ebels, V. Baltz, A.-L. Barra, H. Y. Chen, G. Jakob, S. X. Cao, J. Sinova, O. Gomonay, R. Lebrun, and M. Kläui, "Anisotropic long-range spin transport in canted antiferromagnetic orthoferrite YFeO₃," *Nature Communications* **13** (2022), 10.1038/s41467-022-33520-5.
 - ¹³⁴C. Song, H. Bai, Z. Zhou, L. Han, H. Reichlova, J. H. Dil, J. Liu, X. Chen, and F. Pan, "Altermagnets as a new class of functional materials," *Nature Reviews Materials*, 1–13 (2025).
 - ¹³⁵O. Gomonay, V. Kravchuk, R. Jaeschke-Ubiergo, K. Yershov, T. Jungwirth, L. Šmejkal, J. v. d. Brink, and J. Sinova, "Structure, control, and dynamics of altermagnetic textures," *npj Spintronics* **2**, 35 (2024).
 - ¹³⁶R. Zarzuela, R. Jaeschke-Ubiergo, O. Gomonay, L. Šmejkal, and J. Sinova, "Transport theory and spin-transfer physics in d-wave altermagnets," *Physical Review B* **111**, 064422 (2025).
 - ¹³⁷O. Amin, A. Dal Din, E. Golias, Y. Niu, A. Zakharov, S. Fromage, C. Fields, S. Heywood, R. Cousins, F. Maccherozzi, *et al.*, "Nanoscale imaging and control of altermagnetism in MnTe," *Nature* **636**, 348–353 (2024).
 - ¹³⁸R. Hoyer, P. P. Stavropoulos, A. Razpopov, R. Valentí, L. Šmejkal, and A. Mook, "Altermagnetic splitting of magnons in hematite α -Fe₂O₃," *Physical Review B* **112**, 064425 (2025).
 - ¹³⁹E. Galindez-Ruales, R. Gonzalez-Hernandez, C. Schmitt, S. Das, F. Fuhrmann, A. Ross, E. Golias, A. Akashdeep, L. Lünenbürger, E. Baek, W. Yang, L. Šmejkal, V. Krishna, R. Jaeschke-Ubiergo, J. Sinova, A. Rothschild, C. You, G. Jakob, and M. Kläui, "Revealing the altermagnetism in hematite via xmed imaging and anomalous hall electrical transport," *Advanced Materials* **37**, e05019 (2025).
 - ¹⁴⁰F. Garcia-Gaitan, A. Kefayati, J. Q. Xiao, and B. K. Nikolić, "Magnon spectrum of altermagnets beyond linear spin wave theory: Magnon-magnon interactions via time-dependent matrix product states versus atomistic spin dynamics," *Physical Review B* **111**, L020407 (2025).
 - ¹⁴¹V. V. Kruglyak, S. O. Demokritov, D. Grundler, B. Hillebrands, M. P. Kostylev, C. Sandweg, A. Slavin, R. L. Stamps, D. L. Vainchtein, B. V. Waeyenberge, and C. Wiese, "The 2024 magnonics roadmap," *J. Phys. D: Appl. Phys.* **57** (2024).
 - ¹⁴²L. N. Kapoor, S. Mandal, P. C. Adak, M. Patankar, S. Manni, A. Thamizhavel, and M. M. Deshmukh, "Observation of standing spin waves in a van der waals magnetic material," *Advanced Materials* **33** (2020), 10.1002/adma.202005105.

- ¹⁴³B. Hussain and M. G. Cottam, “Dipole-exchange spin waves in two-dimensional van der Waals ferromagnetic films and stripes,” *Journal of Physics: Condensed Matter* **34**, 445801 (2022).
- ¹⁴⁴F. Schulz, K. Litzius, L. Powalla, M. T. Birch, R. A. Gallardo, S. Satheesh, M. Weigand, T. Scholz, B. V. Lotsch, G. Schütz, M. Burghard, and S. Wintz, “Direct observation of propagating spin waves in the 2d van der Waals ferromagnet Fe_5GeTe_2 ,” *Nano Letters* **23**, 10126–10131 (2023).
- ¹⁴⁵H. Wang, H. Lu, Z. Guo, A. Li, P. Wu, J. Li, W. Xie, Z. Sun, P. Li, H. Damas, A. M. Friedel, S. Migot, J. Ghanbaja, L. Moreau, Y. Fagot-Revurat, S. Petit-Watelot, T. Hauet, J. Robertson, S. Mangin, W. Zhao, and T. Nie, “Interfacial engineering of ferromagnetism in wafer-scale van der Waals Fe_4GeTe_2 far above room temperature,” *Nature Communications* **14**, 2483 (2023).
- ¹⁴⁶H. Liu, H. Malissa, R. M. Stolley, J. Singh, M. Groesbeck, H. Popli, M. Kavand, S. K. Chong, V. V. Deshpande, J. S. Miller, C. Boehme, and Z. V. Vardeny, “Spin wave excitation, detection, and utilization in the organic-based magnet, $\text{V}(\text{TCNE})_x$ (TCNE = Tetracyanoethylene),” *Advanced Materials* **32** (2020), 10.1002/adma.202002663.
- ¹⁴⁷B. McCullian, M. Chilcote, V. Bhallamudi, C. Purser, E. Johnston-Halperin, and P. Hammel, “Broadband optical detection of ferromagnetic resonance from the organic-based ferrimagnet $\text{V}(\text{TCNE})_x$ using N-V centers in diamond,” *Physical Review Applied* **14** (2020), 10.1103/physrevapplied.14.024033.
- ¹⁴⁸P. Li, T. Liu, H. Chang, A. Kalitsov, W. Zhang, G. Csaba, W. Li, D. Richardson, A. DeMann, G. Rimal, *et al.*, “Spin-orbit torque-assisted switching in magnetic insulator thin films with perpendicular magnetic anisotropy,” *Nature Communications* **7**, 12688 (2016).
- ¹⁴⁹5G tools for RF Wireless. “Frequency bands for 5G NR,” (2025).
- ¹⁵⁰Infineon60GHz, “60 ghz radar sensors for automotive applications,” <https://www.infineon.com/products/sensor/radar-sensors/radar-sensors-for-automotive/60ghz-radar> (2024).
- ¹⁵¹IB-Lenhardt, “Automotive radar,” <https://ib-lenhardt.com/kb/automotive-radar> (2024).
- ¹⁵²P. Wachter, “Chapter 19 europium chalcogenides: Euo, eus, euse and eute,” in *Alloys and Intermetallics* (Elsevier, 1979) p. 507–574.
- ¹⁵³M. Schlipf, M. Betzinger, M. Ležaić, C. Friedrich, and S. Blügel, “Structural, electronic, and magnetic properties of the europium chalcogenides: A hybrid-functional dft study,” *Physical Review B* **88**, 094433 (2013).
- ¹⁵⁴W. Boncher, H. Dalafu, N. Rosa, and S. Stoll, “Europium chalcogenide magnetic semiconductor nanostructures,” *Coordination Chemistry Reviews* **289–290**, 279–288 (2015).
- ¹⁵⁵T. Dietl, A. Bonanni, and H. Ohno, “Families of magnetic semiconductors — an overview,” *Journal of Semiconductors* **40**, 080301 (2019).
- ¹⁵⁶I. Kolokolov, V. S. L’vov, and A. Pomyalov, “Precritical anomalous scaling and magnetization temperature dependence in cubic ferromagnetic crystals,” *Physical Review B* **111** (2025), 10.1103/physrevb.111.104433.
- ¹⁵⁷S. von Molnár and A. W. Lawson, “Ferromagnetic and paramagnetic resonance in eus,” *Physical Review* **139**, A1280–A1285 (1965).
- ¹⁵⁸M. C. Franzblau, G. E. Everett, and A. W. Lawson, “Magnetocrystalline anisotropy of europium sulfide,” *Physical Review* **164**, 466–472 (1967).
- ¹⁵⁹R. F. Brown, A. W. Lawson, and G. E. Everett, “Magnetocrystalline anisotropy of europium selenide,” *Physical Review* **172**, 559–564 (1968).
- ¹⁶⁰J. W. Battles and G. E. Everett, “Temperature dependence of the antiferromagnetic resonance linewidth in eute,” *Journal of Applied Physics* **40**, 1240–1240 (1969).
- ¹⁶¹D. E. Eastman, “Temperature dependence of the resonance linewidth in euo,” *Physics Letters A* **28**, 136–137 (1968).
- ¹⁶²S. Kunii, S. Maekawa, and E. Hirahara, “Temperature and frequency dependences of line width of antiferromagnetic resonance in europium telluride,” *Journal of the Physical Society of Japan* **37**, 57–62 (1974).
- ¹⁶³J. Dillon, J. F. and C. E. Olsen, “Ferromagnetic resonance of euo,” *Physical Review* **135**, A434–A439 (1964).
- ¹⁶⁴M. X. Aguilar-Pujol, S. Catalano, C. González-Orellana, W. Skowroński, J. M. Gomez-Perez, M. Ilyin, C. Rogero, M. Gobbi, L. E. Hueso, and F. Casanova, “Magnon currents excited by the spin seebeck effect in ferromagnetic eus thin films,” *Physical Review B* **108** (2023), 10.1103/physrevb.108.224420.
- ¹⁶⁵V. B. Bobkov and I. V. Zavislyak, “Equilibrium state and magnetic permeability tensor of the epitaxial ferrite films,” *Phys. Status Solidi A* **164**, 791–804 (1997).
- ¹⁶⁶E. G. Spencer, R. C. LeCraw, and A. M. Clogston, “Low-temperature linewidth maximum in yttrium iron garnet,” *Physical Review Letters* **3**, 32–33 (1959).
- ¹⁶⁷G. A. Melkov, A. D. Dzyapko, A. V. Chumak, and A. N. Slavin, “Two-magnon relaxation reversal in ferrite spheres,” *Journal of Experimental and Theoretical Physics* **99**, 1193–1200 (2004).
- ¹⁶⁸J. F. Dillon and J. W. Nielsen, “Effects of rare earth impurities on ferrimagnetic resonance in yttrium iron garnet,” *Phys. Rev. Lett.* **3**, 30–31 (1959).
- ¹⁶⁹E. G. Spencer, R. C. LeCraw, and R. C. Linares, “Low-temperature ferromagnetic relaxation in yttrium iron garnet,” *Physical Review* **123**, 1937–1938 (1961).
- ¹⁷⁰P. Pincus, M. Sparks, and R. C. LeCraw, “Ferromagnetic relaxation. ii. the role of four-magnon processes in relaxing the magnetization in ferromagnetic insulators,” *Physical Review* **124**, 1015–1018 (1961).
- ¹⁷¹R. M. White and M. Sparks, “Ferromagnetic relaxation. III. Theory of instabilities,” *Physical Review* **130**, 632–638 (1963).
- ¹⁷²T. Kasuya and R. C. LeCraw, “Relaxation mechanisms in ferromagnetic resonance,” *Physical Review Letters* **6**, 223–225 (1961).
- ¹⁷³O. Klein, V. Charbois, V. V. Naletov, and C. Fermon, “Direct measurement of the spin–lattice relaxation in a ferromagnet,” *Journal of Magnetism and Magnetic Materials* **272–276**, E1027–E1028 (2004).
- ¹⁷⁴V. V. Naletov, G. de Loubens, V. Charbois, O. Klein, V. S. Tiberkevich, and A. N. Slavin, “Ferromagnetic resonance spectroscopy of parametric magnons excited by a four-wave process,” *Physical Review B* **75**, 140405(R) (2007).
- ¹⁷⁵A. Rückriegel, P. Kopietz, D. A. Bozhko, A. A. Serga, and B. Hillebrands, “Magnetoelastic modes and lifetime of magnons in thin yttrium iron garnet films,” *Physical Review B* **89** (2014), 10.1103/physrevb.89.184413.
- ¹⁷⁶S. Streib, N. Vidal-Silva, K. Shen, and G. E. W. Bauer, “Magnon-phonon interactions in magnetic insulators,” *Physical Review B* **99** (2019), 10.1103/physrevb.99.184442.
- ¹⁷⁷M. Müller, J. Weber, S. Goennenwein, S. V. Kusminskiy, R. Gross, M. Althammer, and H. Huebl, “Temperature dependence of the magnon-phonon interaction in hybrids of high-overtone bulk acoustic resonators with ferromagnetic thin films,” *Physical Review Applied* **21**, 034032 (2024).
- ¹⁷⁸Y. Ba, J. Puebla, K. Yamamoto, Y. Hwang, L. Liao, S. Maekawa, O. Klein, and Y. Otani, “Nonreciprocal resonant surface acoustic wave absorption in $\text{Y}_3\text{Fe}_5\text{O}_{12}$,” *Physical Review B* **111**, 104401 (2025).
- ¹⁷⁹M. Cherkasskii, F. Engelhardt, M. Müller, J. Weber, M. Althammer, S. T. B. Goennenwein, H. Huebl, and S. Viola Kusminskiy, “Theory of polarization-dependent phonon pumping in ferromagnetic/non-magnetic bilayers,” *Journal of Applied Physics* **138**, 043906 (2025).
- ¹⁸⁰T. Makiuchi, T. Hioki, H. Shimizu, K. Hoshi, M. Elyasi, K. Yamamoto, N. Yokoi, A. A. Serga, B. Hillebrands, G. E. W. Bauer, and E. Saitoh, “Persistent magnetic coherence in magnets,” *Nature Materials* **23**, 627–632 (2024).
- ¹⁸¹J. Bensmann, R. Schmidt, K. O. Nikolaev, D. Raskhodchikov, S. Choudhary, R. Bhardwaj, S. Taheriniya, A. Varri, S. Niehues, A. El Kadri, J. Kern, W. H. P. Pernice, S. O. Demokritov, V. E. Demidov, S. Michaelis de Vasconcellos, and R. Bratschkisch, “Dispersion-tunable low-loss implanted spin-wave waveguides for large magnonic networks,” *Nature Materials* (2025), 10.1038/s41563-025-02282-y.
- ¹⁸²H. Suhl, “The theory of ferromagnetic resonance at high signal powers,” *Journal of Physics and Chemistry of Solids* **1**, 209–227 (1957).
- ¹⁸³J. J. Burnett, A. Bengtsson, M. Scigliuzzo, D. Niepce, M. Kudra, P. Delsing, and J. Bylander, “Decoherence benchmarking of superconducting qubits,” *npj Quantum Information* **5** (2019), 10.1038/s41534-019-0168-5.
- ¹⁸⁴J. B. Youssef, N. Beaulieu, R. Schlitz, D. Petrosyan, M. Lammel, and W. Legrand, “Low-temperature-compatible iron garnet films grown by liquid phase epitaxy,” *arXiv* (2025), 10.48550/ARXIV.2509.06242.
- ¹⁸⁵A. R. Will-Cole, J. L. Hart, V. Lauter, A. Grutter, C. Dubs, M. Lindner, T. Reimann, N. R. Valdez, C. J. Pearce, T. C. Monson, J. J. Cha, D. Heiman, and N. X. Sun, “Negligible magnetic losses at low temperatures in liquid phase epitaxy grown $\text{Y}_3\text{Fe}_5\text{O}_{12}$ films,” *Physical Review Materials* **7**, 054411 (2023).
- ¹⁸⁶S. Guo, D. Russell, J. Lanier, H. Da, P. C. Hammel, and F. Yang, “Strong on-chip microwave photon–magnon coupling using ultralow-damping epitaxial $\text{Y}_3\text{Fe}_5\text{O}_{12}$ films at 2K,” *Nano Letters* **23**, 5055–5060 (2023).
- ¹⁸⁷W. Legrand, Y. Kemna, S. Schären, H. Wang, D. Petrosyan, L. Holder, R. Schlitz, M. H. Aguirre, M. Lammel, and P. Gambardella, “Lattice-

- tunable substituted iron garnets for low-temperature magnonics,” *Advanced Functional Materials*, 2503644 (2025).
- ¹⁸⁸S. Rani, X. Cao, A. E. Baptista, A. Hoffmann, and W. Pfaff, “High-dynamic-range quantum sensing of magnons and their dynamics using a superconducting qubit,” *Physical Review Applied* **23** (2025), 10.1103/6dmm-mnxd.
- ¹⁸⁹C. Dubs, O. Surzhenko, R. Linke, A. Danilewsky, U. Brückner, and J. Delilith, “Sub-micrometer yttrium iron garnet LPE films with low ferromagnetic resonance losses,” *Journal of Physics D: Applied Physics* **50**, 204005 (2017).
- ¹⁹⁰C. Dubs, O. Surzhenko, R. Thomas, J. Osten, T. Schneider, K. Lenz, J. Grenzer, R. Hübner, and E. Wendler, “Low damping and microstructural perfection of sub-40nm-thin yttrium iron garnet films grown by liquid phase epitaxy,” *Physical Review Materials* **4**, 024416 (2020).
- ¹⁹¹J. Ding, T. Liu, H. Chang, and M. Wu, “Sputtering growth of low-damping yttrium-iron-garnet thin films,” *IEEE Magn. Lett.* **11**, 1–5 (2020).
- ¹⁹²F. Heyroth, C. Hauser, P. Trempler, P. Geyer, F. Syrowatka, R. Dreyer, S. Ebbinghaus, G. Woltersdorf, and G. Schmidt, “Monocrystalline free-standing three-dimensional yttrium-iron-garnet magnon nanoresonators,” *Physical Review Applied* **12**, 054031 (2019).
- ¹⁹³L. J. Cornelissen, J. Liu, R. A. Duine, J. B. Youssef, and B. J. van Wees, “Long-distance transport of magnon spin information in a magnetic insulator at room temperature,” *Nature Physics* **11**, 1022–1026 (2015).
- ¹⁹⁴M. C. Onbasli, A. Kehlberger, D. H. Kim, G. Jakob, M. Kläui, A. V. Chumak, B. Hillebrands, and C. A. Ross, “Pulsed laser deposition of epitaxial yttrium iron garnet films with low Gilbert damping and bulk-like magnetization,” *APL Materials* **2**, 106102 (2014).
- ¹⁹⁵C. Hahn, V. V. Naletov, G. de Loubens, O. Klein, O. d’Allivy Kelly, A. Anane, R. Bernard, E. Jacquet, P. Bortolotti, V. Cros, J. L. Prieto, and M. Muñoz, “Measurement of the intrinsic damping constant in individual nanodisks of $Y_3Fe_5O_{12}|Pt$,” *Applied Physics Letters* **104**, 152410 (2014).
- ¹⁹⁶N. Askarzadeh and H. Shokrollahi, “Advances in yig thin films: Deposition strategies and substrate effects,” *Results in Chemistry* **16**, 102390 (2025).
- ¹⁹⁷V. Danilov, D. Lyfar’, Y. V. Lyubon’ko, A. Y. Nechiporuk, and S. Ryabchenko, “Low-temperature ferromagnetic resonance in epitaxial garnet films on paramagnetic substrates,” *Sov. Phys. J.* **32**, 276–280 (1989).
- ¹⁹⁸P. P. Deen, O. Florea, E. Lhotel, and H. Jacobsen, “Updating the phase diagram of the archetypal frustrated magnet $Gd_3Ga_5O_{12}$,” *Physical Review B* **91**, 014419 (2015).
- ¹⁹⁹O. A. Petrenko, C. Ritter, M. Yethiraj, and D. McK Paul, “Investigation of the low-temperature spin-liquid behavior of the frustrated magnet gadolinium gallium garnet,” *Phys. Rev. Lett.* **80**, 4570–4573 (1998).
- ²⁰⁰P. Schiffer, A. P. Ramirez, D. A. Huse, and A. J. Valentino, “Investigation of the field induced antiferromagnetic phase transition in the frustrated magnet: Gadolinium gallium garnet,” *Phys. Rev. Lett.* **73**, 2500–2503 (1994).
- ²⁰¹D. Schmall, R. O. Serha, J. Panda, A. A. Voronov, C. Dubs, M. Urbánek, and A. V. Chumak, “Elimination of substrate-induced ferromagnetic resonance linewidth broadening in the epitaxial system YIG-GGG by microstructuring,” *Low Temperature Physics* **51**, 724–730 (2025).
- ²⁰²A. Sposito, T. C. May-Smith, G. B. G. Stenning, P. A. J. de Groot, and R. W. Eason, “Pulsed laser deposition of high-quality μm -thick YIG films on YAG,” *Optical Materials Express* **3**, 624–632 (2013).
- ²⁰³A. Krysztofik, S. Özoğlu, R. D. McMichael, and E. Coy, “Effect of strain-induced anisotropy on magnetization dynamics in $Y_3Fe_5O_{12}$ films recrystallized on a lattice-mismatched substrate,” *Scientific Reports* **11** (2021), 10.1038/s41598-021-93308-3.
- ²⁰⁴K. Enke, J. Fleischhauer, W. Gunsser, P. Hansen, S. Nomura, W. Tolksdorf, G. Winkler, and U. Wolfmaier, “Part A: Garnets and Perovskites,” in *Landolt-Börnstein - Group III Condensed Matter*, Vol. 12A, edited by K.-H. Hellwege and A. M. Hellwege (Springer-Verlag, 1978) p. 482–494.
- ²⁰⁵T. Yoshimoto, T. Goto, K. Shimada, B. Iwamoto, Y. Nakamura, H. Uchida, C. A. Ross, and M. Inoue, “Static and dynamic magnetic properties of single-crystalline yttrium iron garnet films epitaxially grown on three garnet substrates,” *Adv. Electron. Mater.* **5** (2019), 10.1002/aelm.201900380.
- ²⁰⁶J. E. Abrão, D. Weltens, R. Mansell, S. van Dijken, and L. Flajšman, “Spin-wave propagation at low temperatures in YIG thin films on YSGG substrates,” *arXiv* (2025), 10.48550/ARXIV.2510.04330.